

JAMES COOK UNIVERSITY

SCHOOL OF ENGINEERING

EG4011/2

Quantifying the Rate of Three
Dimensional Consolidation

Samantha Rose Thomas

Thesis submitted to the School of Engineering in partial fulfilment
of the requirements for the degree of

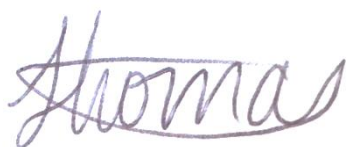
Bachelor of Engineering with Honours
(Civil)

October, 31st 2013

Statement of Access

I, the undersigned, author of this work, understand that James Cook University may make this thesis available for use within the University Library and, via the Australian Digital Theses network, for use elsewhere.

I understand that, as an unpublished work, a thesis has significant protection under the Copyright Act and I do not wish to place any further restriction on access to this work.



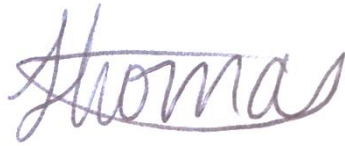
30/10/13

Samantha Thomas

Date

Declaration of Sources

I declare that this thesis is my own work and has not been submitted in any form for another degree or diploma at any university or other institution of tertiary education. Information derived from the published or unpublished work of others has been acknowledged in the text and a list of references is given.



30/10/13

Samantha Thomas

Date

Abstract

Geotechnical engineers generally quantify the coefficient of consolidation using the one dimensional consolidation theory of Terzaghi (1925), assuming drainage and strain occurs in the vertical plane only. As many field scenarios actually experience drainage in both the vertical and horizontal directions (two and three dimensional consolidation), the rate of consolidation that occurs in these situations is greater than that assumed when using one dimensional consolidation theory.

The primary objective of this thesis was to quantify the rate of three dimensional consolidation. This was achieved through the derivation of an analytical solution, and validation via experimental investigation.

The analytical solution derived allowed average consolidation ($U-T$) curves to be developed for a variety of radius/height (R/H) values. Through a series of solution processes, a relation was made between the time factor of consolidation and the coefficient of horizontal consolidation (c_h). Modifications to the graphical methods of Casagrande and Taylor were proposed, allowing a curve fitting procedure for varying R/H values.

Experimental investigation was undertaken on kaolin clay for both one dimensional and axisymmetric three dimensional consolidation. Results showed a horizontal coefficient of consolidation approximately one to four times greater than that of the vertical coefficient of consolidation.

Furthermore, a comparison of creep obtained from the one dimensional and axisymmetric three dimensional consolidation apparatus was completed, with results showing an increase in creep after the preconsolidation pressure was reached. The creep after this point for three dimensional consolidation however, was much greater than that of one dimensional consolidation.

Finally, the compression-recompression curves were analysed for both one and three dimensional consolidation. A similar compression index was experienced between one and three dimensional consolidation, however a smaller recompression index resulted for three dimensional samples.

Acknowledgements

This thesis was conducted under the supervision of Dr Julie Lovisa. I would like to thank Julie for the support and guidance she has provided me over the duration of this thesis. I am extremely grateful for the large amount of time she spared to meet on a regular basis, and the understanding she provided.

I would also like to thank Associate Professor Nagaratnam Sivakugan, who always had time to spare to consolidate my understanding, or to answer any question I had.

Furthermore, I wish to express my gratitude to Warren O'Donnell for building our apparatus, and in general, for the numerous hours he spent with us in the laboratory.

On a more personal note, I would like to thank my parents and sister for the support they have provided me, not only over the past year of thesis, but throughout my university degree.

Table of Contents

Chapter 1: Introduction	1
1.1 General	1
1.2 Problem Definition	1
1.3 Project Objectives.....	2
Chapter 2: Literature Review	3
2.1 Soil Property Overview	3
2.1.1 Nature of Clays.....	3
Permeability of a Soil	3
Anisotropy of a Soil.....	4
2.2 Consolidation Theory	4
2.2.1 Elastic Settlement and Primary and Secondary Consolidation.....	4
2.2.2 Time Period of Consolidation	6
2.3 One-Dimensional Consolidation	6
2.3.1 Total Consolidation Settlement (s_c).....	6
2.3.2 Consolidation Testing.....	8
2.3.3 Void-Log σ_v' Plot.....	9
Preconsolidation Pressure (σ_p'), Overconsolidated Clay and Normally Consolidated Clay	10
2.3.4 Terzaghi's One Dimensional Consolidation Theory	11
Modified Analytical Solution to Terzaghi's Differential Equation.....	14
Degree of Consolidation.....	14
Average Degree of Consolidation	15
2.4 Calculating Coefficient of Consolidation (c_v).....	17
Casagrande's Log Time Method	18
Taylor's Square Root of Time method	19
Other Methods to Calculate the Coefficient of Consolidation	20
2.5 Two and Three Dimensional Consolidation	21
2.5.1 Two and Three Dimensional Consolidation Theories	21
Vertical Drains.....	22
Numerical Models	23
2.6 Application – Land Reclamation.....	23
2.6.1 Port of Brisbane, Queensland, Australia	24
Chapter 3: Analytical Solution of Three Dimensional Consolidation.....	26
3.1 General	26
3.2 Extension from One Dimension to Three Dimensions.....	26
3.3 Summary.....	31
Chapter 4: Experimental Investigation Methodology	32
4.1 Overview	32
4.2 Soil Properties	32
4.2.1 Determination of Soil Parameters.....	32
4.3 Tall Oedometer for Sample Preparation.....	33
4.4 Homogeneity between samples	34
4.5 One Dimensional Consolidation.....	34
4.6 Three Dimensional Consolidation	35
4.7 Scanning Electron Microscope (SEM).....	36

4.8	Summary.....	37
Chapter 5: Quantifying the Horizontal Coefficient of Consolidation (c_h) 38		
5.1	General	38
5.2	Experimental Results of Coefficient of Consolidation (c_v) from One Dimensional Settlement-time plots.....	38
5.3	Coefficient of Equivalent Three Dimensional Consolidation ($c_{3Dequiv}$)	39
5.3.1	Modified Taylor's and Casagrande's Method	40
	Taylor's Method	40
	Casagrande's Method	40
5.4	Time Factor of Three Dimensional Consolidation ($T_{50,3D}$).....	41
	Casagrande's Method	41
	Taylor's Method	42
5.4.1	Finding $T_{50,3D}$ – An example using Casagrande's Method	43
5.4.2	Experimental Results of the Time Factor of Three Dimensional Consolidation ($T_{50,3D}$).....	45
5.5	Determining the Horizontal Coefficient of Consolidation	46
5.5.1	Method to determine the Radial Factor with an input of time factor using MATLAB	48
5.5.2	Comparison Between Horizontal Coefficient of Consolidation of Casagrande's and Taylor's Method	48
5.5.3	Comparison Between Horizontal Coefficient of Consolidation and Vertical Coefficient of Consolidation	49
	Casagrande's Method	49
	Taylor's Method	50
5.5.4	Comparison with Literature.....	51
5.6	Comparison between Analytical and Experimental Average Degree of Consolidation ($U-T$) Curves	51
5.7	Scanning Electron Microscope (SEM) Images – Analysing Particle Orientation..	52
5.7.1	SEM Image – After Sample Preparation	52
5.7.2	SEM Image – After Standard Oedometer.....	53
5.8	Summary.....	55
Chapter 6: Further Experimental Investigation 56		
6.1	Verification of the Coefficient of Consolidation through Falling Head Permeability Testing	56
6.2	Creep Estimation	57
6.2.1	Comparison with Literature.....	57
6.3	Void-log σ_v' Curve.....	58
6.4	Summary.....	59
Chapter 7: Summary, Conclusions and Recommendations..... 61		
7.1	Calculation of the Horizontal Coefficient of Consolidation.....	61
7.2	Creep Estimation	62
7.3	Compression-Recompression Curves.....	62
References 63		

List of Figures

Figure 2.1: Settlement-time Relationship	5
Figure 2.2: Change in Effective Stress and Pore Water Pressure with Time	5
Figure 2.3: Standard One Dimensional Consolidation Oedometer.....	8
Figure 2.4: Void-log σ'_v plot – (a) definitions (b) virgin consolidation line (Sivakugan and Das 2009)	10
Figure 2.5: Degree of Consolidation Chart (U - Z - T Variation)	15
Figure 2.6: Average Degree of Consolidation Chart (U – T chart).....	16
Figure 2.7: Influence of Strain Profile on Rate of Consolidation Settlement (Duncan 1993) ..	17
Figure 2.8: Casagrande’s Log Time Method (using experimental results of 155 kPa loading increment)	19
Figure 2.9: Taylor’s Square Root of Time Method, (using experimental results of 618 kPa increment)	20
Figure 2.10: Aerial view of Land Reclamation at the Port of Brisbane (Ganesalingam et al. 2012a)	25
Figure 3.1: Average Degree of Consolidation Curves for Varying R/H Ratios (Lovisa et al. 2014)	28
Figure 3.2: Quantifying Anisotropy using Modified Time Factors – Casagrande’s Method (Lovisa et al. 2014)	30
Figure 3.3: Quantifying Anisotropy using Modified Time Factors – Taylor’s Method (Lovisa et al. 2014)	30
Figure 4.1: Tall Oedometer Schematic (Lovisa and Sivakugan)	33
Figure 4.2: Orientation of Permeability Consolidation Samples	35
Figure 4.3: Three Dimensional Consolidation Apparatus Schematic	36
Figure 5.1: Vertical Coefficient of Consolidation - Comparison between Casagrande’s and Taylor’s Graphical Method.....	39
Figure 5.2: Modified vs. Non-Modified Coefficient of Consolidation Values for a Three Dimensional Sample	41
Figure 5.3: Three Dimensional Casagrande’s Method Time Factors Using Experimental Data	45
Figure 5.4: Three Dimensional Taylor’s Method Time Factors Using Experimental Data...	46
Figure 5.5: Determining the Horizontal Coefficient of Consolidation	47
Figure 5.6: Comparison of Horizontal Coefficient of Consolidation obtained using Casagrande’s and Taylor’s Method	49
Figure 5.7: Comparison between the Horizontal Coefficient of Consolidation and Vertical Coefficient of Consolidation – Casagrande’s Method	50

Figure 5.8: Comparison of Horizontal Coefficient of Consolidation obtained using Casagrande's and Taylor's Method	50
Figure 5.9: Average Degree of Consolidation (U - T) Curves for One and Three Dimensional Consolidation – Verification of Analytical Solution Using Experimental Data	52
Figure 5.10: SEM Image – After Tall Oedometer (Top View).....	53
Figure 5.11: SEM Image – After Standard Oedometer for One Dimensional Horizontally Cut Sample	54
Figure 5.12: SEM Image – After Standard Oedometer on a Vertically Cut Sample.	54
Figure 5.13: SEM Image – After Standard Oedometer of a Three Dimensional Sample	55
Figure 6.1: Comparison Between the Coefficient of Consolidation obtained from Taylor's and Casagrande's Method, and the Direct Determination of Permeability.....	56
Figure 6.2: Comparison of Coefficient of Secondary Consolidation (c_α) for Three Dimensional and One Dimensional Consolidation	57
Figure 6.3: Void- $\log \sigma'_v$ Curve for One Dimensional Consolidation.....	58
Figure 6.4: Void- $\log \sigma'_v$ Curve for Three Dimensional Consolidation	59

List of Tables

Table 3.1: Modified curve-fitting parameters (Lovisa et al. 2014)	29
Table 4.1: Properties of Kaolin Clay	32
Table 4.2: Tests undertaken for Soil Classification	32
Table 5.1: Corrections of Taylor's and Casagrande's Method to Three Dimensional Consolidation Settlement-time plots	40
Table 6.1: Compression Index and Recompression Index Values for Experimental Results	59
Table 7.1: Boundary and Initial Conditions of One and Two-Way Drainage	67
Table 7.2: Solution Process for Terzaghi's Differential Equation	68

List of Symbols

γ_w	Unit weight of water
$\Delta\sigma$	Change in total stress
$\Delta\sigma'$	Change in effective stress
$\Delta\sigma_v$	Change in applied stress to the consolidating layer
Δe	Change in void ratio
ΔH	Decrease in thickness of the consolidating layer
Δu	Change in excess pore water
Δu_0	Change in initial excess pore water
ρ_s	Soil particle density
σ	Total Stress
$\sigma'_{average}$	Average effective stress throughout consolidation
σ'	Effective stress
σ_p'	Preconsolidation pressure
σ'_v	Vertical effective stress
σ'_{v0}	Initial vertical effective stress
B	Taylor power
C_c	Compression index
c_h	Horizontal coefficient of consolidation
C_r	Recompression index
c_v	Vertical coefficient of consolidation
$c_{3D equiv}$	Equivalent three dimensional coefficient of consolidation
C_x	Horizontal coefficient of consolidation
C_z	Vertical coefficient of consolidation
c_α	Secondary consolidation/creep
d	Depth
D	Constrained modulus

e	Void ratio
E	Young's modulus
e_0	Initial void ratio
f_c	Casagrande Factor
f_T	Taylor factor
G_s	Specific gravity of the soil grains
H	Height of consolidating layer
H_0	Initial height of the consolidating layer
H_{50}	Thickness of specimen at 50 % of the loading increment
H_{dr}	Maximum length of drainage path
k	Coefficient of permeability
k_v	Vertical coefficient of permeability
m_v	Coefficient of volume compressibility
r	Radial component
R	Radius
s_c	Consolidation settlement
$s_{c,total}$	Total consolidation settlement
t	Time after loading
T_{50}	Time factor at 50 % consolidation
T_{90}	Time factor at 90 % consolidation
t_{50}	Time for 50 % consolidation
t_{90}	Time for 90 % consolidation
T^*	Modified time factor
u	Pore water pressure
U_{avg}	Average degree of consolidation
U_z	Degree of consolidation
$U-T$	Average consolidation-time

ν	Poisson's ratio
w	Water content
X	Domain
z	Depth below top of clay
Z	Depth factor

Chapter 1: Introduction

1.1 General

Consolidation is the compression of a soil stratum that occurs due to the application of stress, and as a result of the dissipation of water from voids in a saturated soil. Consolidation settlement can result in many problems for structures built upon a consolidating layer, and therefore correct estimation of the magnitude and rate of the settlement is required.

One dimensional consolidation is generally used to quantify the magnitude and rate of consolidation. The theory of Terzaghi (1925), quantifies the time rate of consolidation in one dimension by assuming strains and drainage occur in the vertical plane only. Terzaghi's theory is often used to calculate consolidation settlement. Due to two and three dimensional consolidation conditions in field situations, it is evident that the rate of consolidation settlement that is actually experienced is greater than that obtained using one dimensional consolidation theory (Davis and Poulos 1972). Davis and Poulos (1972) attributed this to the horizontal dissipation of water that occurs in two and three dimensions, resulting in the consolidation of a clay layer occurring more rapidly than predicted by the one dimensional consolidation theory.

1.2 Problem Definition

Two and three dimensional consolidation theories have been developed by Terzaghi (1925) and Rendulic (1937) based on the diffusion theory, and by Biot (1941) in his elastic theory (Razouki and Al-Zayadi (2003); Poulos and Davis (1968)). However, due to the difficulty of these theories and minimal theoretical practical solutions having been obtained, one dimensional consolidation theory is generally used (Davis and Poulos 1972).

The determination of two and three dimensional consolidation has many field applications. This includes land reclamation, with such examples including the Port of Brisbane, Queensland where land reclamation is currently being undertaken. The Port of Brisbane utilises dredged materials as fill, providing both economic and environmental benefit.

Unfortunately, the dredged material is comprised of silts and clays in a slurry form with extremely high water content, resulting in poor drainage properties. The containment bunds are underlain by a Holocene clay layer of up to 30 m in depth, further underlain by an extremely stiff Pleistocene. This results in both the dredged material and in situ material having poor drainage properties and high compressibility (Ganesalingam et al. 2012a).

Due to the limitations in consolidation theory, the estimation of the rate of settlement is difficult, with the time taken for consolidation to be achieved often overestimated. Generally, an increased cost is involved as a result of the overestimated time of settlement. This highlights the importance and necessity of the time rate of two and three dimensional consolidation to be quantified.

1.3 Project Objectives

The primary objective of this thesis is to quantify the rate of three dimensional axisymmetric consolidation. This will be completed through the derivation of an analytical equation and experimental investigation using a new three dimensional axisymmetric consolidation apparatus.

The intended objectives of this study are therefore to:

- Develop a functional three dimensional axisymmetric consolidation apparatus;
- Quantify anisotropy in the coefficient of consolidation of a soil through standard one dimensional consolidation tests of both horizontally and vertically cut samples, and validate by obtaining both vertical and horizontal permeability values in a consolidation cell equipped with permeability capabilities;
- Derive an analytical equation that quantifies the anisotropy of a sample ; and
- Develop design charts of average consolidation curves ($U-T$ curves) for three dimensional axisymmetric consolidation with varying radius to height (R/H) ratios and analysing these with respect to the one dimensional $U-T$ curve.

Furthermore, using the data obtained from experimental investigation of three dimensional axisymmetric consolidation, the secondary objectives are to:

- Compare the rate of secondary consolidation (creep) and the compression and recompression index between one and three dimensional consolidation experimental data.

Chapter 2: Literature Review

2.1 *Soil Property Overview*

A soil is a particulate media consisting of three phases; gas, liquid and soil grains. The gas and liquid are commonly comprised of air and water respectively. The total normal stress present within a soil stratum can be determined by summing the stress on the soil grains (inter-granular/effective stress) and the stress present on the voids within a saturated soil (pore pressure/neutral stress). This is evident in Equation (2.1) where the total normal stress is denoted by σ , the inter-granular/effective stress by σ' and the pore pressure/neutral stress by u (Sivakugan and Das 2009).

$$\sigma = \sigma' + u \quad (2.1)$$

A soil can be classified as either coarse or fine grained. Fine grained soils are further classified into clays or silts, with a grain size less than 0.075 mm as outlined in AS1726-1993. This thesis will focus on clay, a cohesive soil.

2.1.1 **Nature of Clays**

Clay is a fine grained soil that gains shear strength through the bonding of soil particles. Due to electrically charged surfaces, clays are cohesive soils that are plastic in nature and can be moulded when wet. Plasticity is a property exclusive to clays, with silts having no plasticity.

Permeability of a Soil

Permeability of a soil results from the presence of interconnected voids, as water flows from points of high energy to points of low energy (Das 1984). The rate of flow is dictated by Darcy's law, where the flow is directly proportional to the coefficient of permeability (hydraulic conductivity) of the soil. The coefficient of permeability (k) varies with soil type and is dependent on factors including pore size distribution, void ratio, saturation and structure. Due to the smaller particle size, and therefore the presence of a smaller void ratio in clays, a permeability that is one million times smaller is often evident in clays when compared to sands (Coduto 1998). As the dredged materials at the Port of Brisbane are comprised of silts and clays, the poor drainage properties, when compared to sands can be seen. This highlights the benefit of using sands and gravels for land reclamation.

Anisotropy of a Soil

An anisotropic material is one in which the elastic properties depend on the orientation of the sample and often refers to soil structure, soil strength and soil permeability in different directions (Peng 2011). This differs to an isotropic material where the sample will exhibit the same elastic properties in all orientations (Graham and Houlsby 1983).

Anisotropy of clay arises due to two components: inherent anisotropy and stress-induced anisotropy, as outlined by Sivakugan et al. (1993) in describing the undrained strength anisotropy of a clay. Inherent anisotropy refers to the way in which the soil was deposited where a preferred particle orientation occurs. As stated by Graham and Houlsby (1983) the periodic deposition of finer and coarser particle sizes within a natural clay will result in a permeability that is anisotropic. Ti et al. (2009) noted that a soil often shows anisotropic behaviour when subjected to stresses. Stress-induced anisotropy refers to the stress at the end of consolidation where anisotropy results from the direction of loading dependent upon the initial anisotropic stress state (Sivakugan et al. 1993).

2.2 Consolidation Theory

Consolidation is defined as the compression of a soil stratum that occurs due to the application of stress. Within a saturated soil, volume decrease (compression) of the soil occurs as a result of the reduction of the volume of voids through the expulsion of water. As the solid matter and pore water are assumed to be incompressible, the resulting settlement can be attributed solely to this reduction in void volume

2.2.1 Elastic Settlement and Primary and Secondary Consolidation

Total settlement of a soil stratum is the contribution of both primary and secondary consolidation settlement, in addition to an initial elastic settlement. This is represented on a one dimensional settlement-time plot obtained from experimental investigation, evident in Figure 2.1.

Elastic settlement occurs immediately after, and due to the application of load and does not cause a change in moisture content of the soil (Winterkorn and Fang 1990). Consolidation settlement comprises two components: primary consolidation settlement; and secondary consolidation settlement, also referred to as creep.

Primary consolidation settlement is the process of volume reduction that occurs within a soil mass as a stress is applied. Initially when a stress is applied, pore water carries the entire

deviator load ($\Delta\sigma = \Delta u$), producing an excess pore water pressure. The excess pore water pressure gives rise to a hydraulic gradient that results in the dissipation of water from voids (Coduto 1998). The deviator load is transferred to the soil skeleton with the dissipation of pore water, and with time, the soil skeleton will carry the entire deviator load ($\Delta\sigma = \Delta\sigma'$). This process is evident in Figure 2.2.

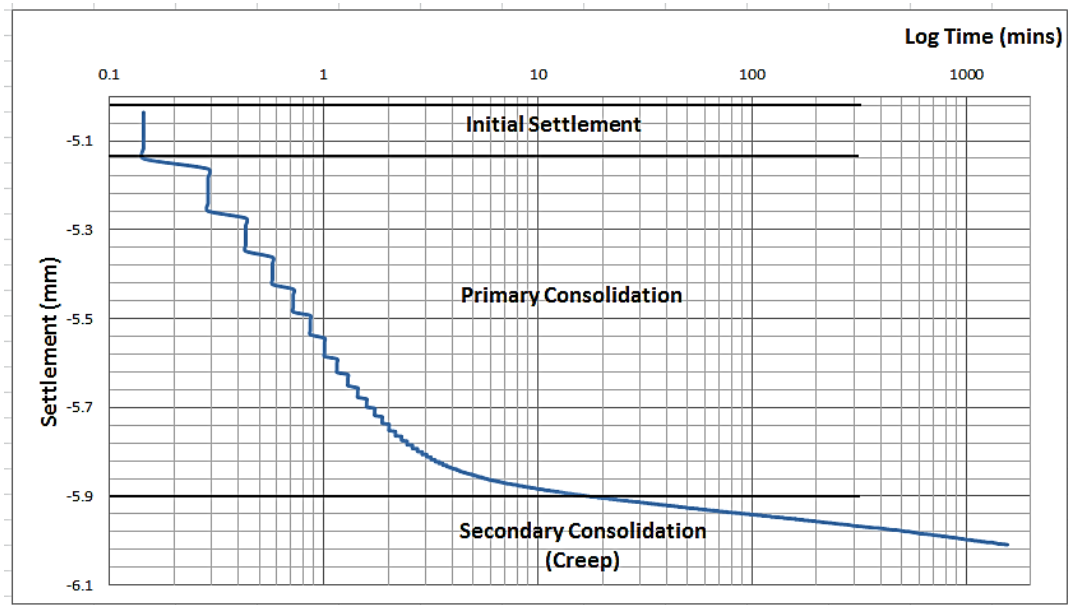


Figure 2.1: Settlement-time Relationship

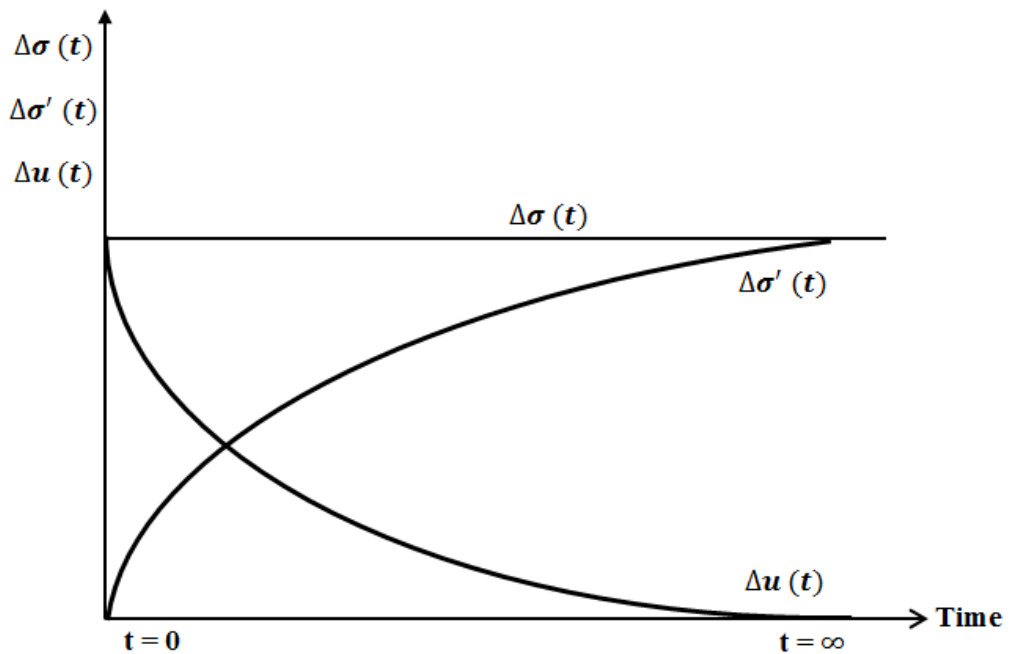


Figure 2.2: Change in Effective Stress and Pore Water Pressure with Time

Secondary consolidation settlement occurs at a constant effective stress and results in additional compression of the soil. It occurs at the end of primary consolidation, and as a result of the rearrangement of the soil fabric of the clay layer (Das 1984).

2.2.2 Time Period of Consolidation

The time period of consolidation is dependent upon many factors, including the permeability of the soil, the drainage conditions of the soil layer and the magnitude of the applied stress (Barnes 1995). Due to the high permeability of a cohesionless soil, total settlement occurs almost immediately. As cohesive soils are less permeable, consolidation is time dependent and total settlement occurs over a prolonged period of time. The time rate of one dimensional consolidation is quantified using Terzaghi's theory, as evident in Section 2.3.4.

Consolidation in the field can occur in one, two or three dimensions. However, calculation of consolidation settlement and time taken for consolidation to occur are often calculated in one dimension. This is due to the availability and simplicity of analytical equations and experimental configurations in one dimension. Two and three dimensional consolidation considers horizontal dissipation of pore pressure, resulting in the consolidation of a clay layer occurring more rapidly than predicted by the one dimensional consolidation theory (Davis and Poulos 1972).

2.3 One Dimensional Consolidation

Consolidation can be considered one dimensional when the applied stress on the soil stratum extends a large width compared to the depth of the soil. This loading situation results in strains and drainage in the vertical plane only.

2.3.1 Total Consolidation Settlement (s_c)

Total consolidation settlement in one dimension is directly related to the change in height to change in void relationship developed by equivalence of the average vertical strain, as evident in Equation (2.2).

$$\frac{\Delta H}{H_0} = \frac{\Delta e}{1 + e_0} \quad (2.2)$$

where:

ΔH = the decrease in thickness of the consolidated clay later

H_0 = the initial height of the clay layer

Δe = the change in void ratio

e_0 = the initial void ratio.

Total consolidation settlement (s_c) can be determined through the relationship of the change in volume of the soil stratum to the coefficient of volume compressibility (m_v) in one dimension by Equation (2.3).

$$s_c = m_v \Delta \sigma' H_0 \quad (2.3)$$

where:

$\Delta \sigma'$ = change in effective stress

m_v = coefficient of volume compressibility

The coefficient of volume compressibility is dependent upon the applied load, and therefore varies within the consolidating layer (Aysen 2002). This method relies on the availability of m_v and requires the stress level to calculate total consolidation settlement (Sivakugan and Das 2009).

The coefficient of volume compressibility can be related to the compression index (C_c) (see Section 2.3.3) in a normally consolidated clay as evident in Equation (2.4). It can also be related to the drained Young's modulus (E), constrained modulus (D) and Poisson's ratio (ν) through Equation (2.5).

$$m_v = \frac{0.434 C_c}{(1 + e_0) \sigma'_{average}} \quad (2.4)$$

where:

$\sigma'_{average}$ = the average effective stress throughout consolidation

$$D = \frac{1}{m_v} = \frac{(1 - \nu)}{(1 + \nu)(1 - 2\nu)} E \quad (2.5)$$

where:

$$D = \frac{\Delta \sigma'}{\left(\frac{\Delta H}{H}\right)} \quad (2.6)$$

A method to calculate total consolidation settlement is obtained by rearranging Equation (2.2) where the change in height of the consolidated clay layer (ΔH) is equivalent to the consolidation settlement (s_c), which can therefore be written as Equation (2.7).

$$s_c = \frac{\Delta e}{1 + e_0} H_0 \quad (2.7)$$

The initial void ratio can be determined through phase relations of a saturated soil as the multiplication of the water content (w) and the specific gravity of the soil grains (G_s), as shown in Equation (2.8).

$$e_0 = wG_s \quad (2.8)$$

To determine the change in void ratio for use within Equation (2.7), the equations outlined in Section 2.3.3 can be used, dependent upon whether the soil is normally consolidated or overconsolidated.

2.3.2 Consolidation Testing

One dimensional consolidation is simulated in the laboratory using an oedometer, in order to quantify the coefficient of consolidation, and hence, the magnitude of consolidation settlement. The configuration of the oedometer can be seen in Figure 2.3.

One dimensional consolidation is executed following the procedure outlined in *AS1289.6.6.1-1998: Soil strength and consolidation tests-Determination of the one dimensional consolidation properties of a soil-Standard Method*.

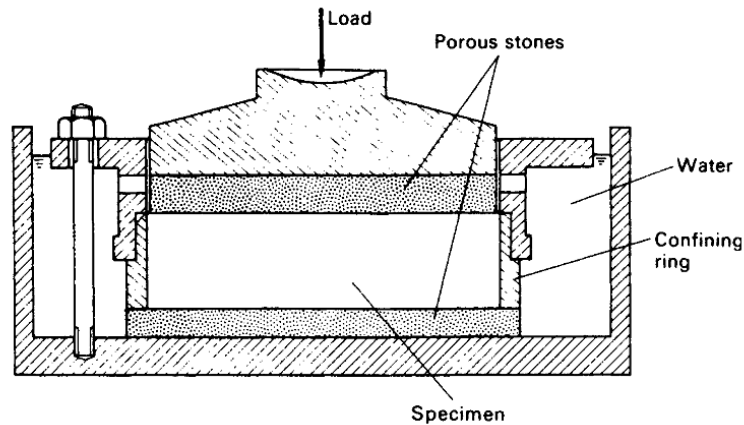


Figure 2.3: Standard One Dimensional Consolidation Oedometer

The specimen is laterally confined by a steel ring with porous stones both above and below the specimen. Due to the lateral confinement, only vertical drainage occurs, which is evident from the top and bottom in a doubly drained state due to two permeable boundaries. To simulate one dimensional consolidation, AS1289.6.6.1-1998 specifies that the minimum

specimen diameter-to-thickness ratio be 3:1, with a minimum diameter and thickness of 50 mm and 15 mm respectively.

The soil specimen, contained within the steel ring, is placed into a consolidation cell filled with water to allow a saturated condition. The sample is loaded vertically, and settlement and time is recorded by means of a dial gauge connected to an electronic monitoring system.

Each load increment is applied for approximately 24 hours or until settlement of the sample is no longer evident. The load is then increased such that the load increment is doubled. This occurs until the maximum required pressure increment is achieved, where the sample can then be unloaded to allow the unloading characteristics of the specimen to be established. At the completion of each load increment, the change in height of the specimen is known, and therefore the void ratio can be indirectly determined using the void ratio-height relationship described in Equation (2.2), with the change in void ratio being determined as per Section 2.3.3.

The resulting settlement-time plot that is obtained from each increment allows the coefficient of consolidation (c_v) to be determined for that increment, as described in Section 2.4. The data obtained from the series of load increments also allows the compression index (C_c), recompression index (C_r), and preconsolidation pressure (σ_p') to be determined by plotting the void ratio at the completion of each load increment against the corresponding load in logarithmic scale. The method to determine these parameters is described in Section 2.3.3.

2.3.3 Void-Log σ_v' Plot

The void-log σ_v' plot is obtained by calculating the void ratio at the end of each load increment during one dimensional consolidation testing and plotting it against the effective vertical stress on a logarithmic scale. A common plot for a saturated clay is evident in Figure 2.4.

As the vertical load increases, it is evident that the void ratio decreases. Initially the curve has a slope equal to the recompression index (C_r) where the soil is overconsolidated. This slope continues until the preconsolidation pressure (σ_p') is reached.

After this point, the slope of the curve follows a linear path, known as the virgin consolidation line (VCL). A clay layer that consolidates along this line is said to be normally consolidated where the curve has a slope equal to the compression index (C_c). As the specimen is unloaded, it is evident that the slope of the curve is again approximately equal to

the recompression index. It is assumed that the slopes of all recompression stages are approximately equal, as suggested by Leonards (1976) (Aysen 2002).

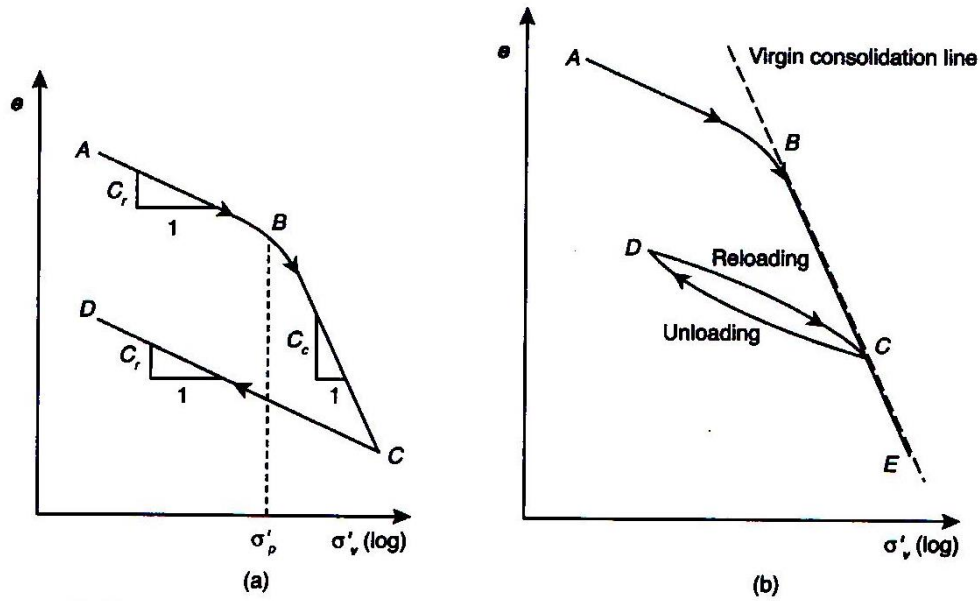


Figure 2.4: Void-log σ_v' plot – (a) definitions (b) virgin consolidation line (Sivakugan and Das 2009)

Preconsolidation Pressure (σ_p'), Overconsolidated Clay and Normally Consolidated Clay

The preconsolidation pressure is defined as the maximum pressure that a consolidating layer has experienced before. A soil stratum can be overconsolidated or normally consolidated which is determined in the laboratory in a one dimensional consolidation test. An overconsolidated clay is a clay that has experienced a past pressure (preconsolidation pressure) greater than that which is being applied. A normally consolidated clay, however, is one in which the load that is being applied is the maximum applied stress that the clay has experienced, and therefore lies on the virgin consolidation line.

The change in void ratio varies depending upon whether the clay is normally consolidated or overconsolidated. An overconsolidated clay results in significantly smaller settlements of a clay layer than would be experienced if the clay was normally consolidated, as the void ratio is smaller resulting in a smaller change in void ratio when a stress is applied (Sivakugan and Das 2009).

The change in void ratio for a normally consolidated clay is evident in Equation (2.9) and results from the movement of a point along the virgin consolidation line, having a slope of the compression index.

$$\Delta e = C_c \log \frac{\sigma_{vo}' + \Delta \sigma'}{\sigma_{vo}'} \quad (2.9)$$

The change in void ratio for an overconsolidated clay depends on whether the applied pressure is less than the preconsolidation pressure ($\sigma_{vo}' + \Delta \sigma' \leq \sigma_p'$), with a relationship evident in Equation (2.10) or whether the applied pressure surpasses that of the preconsolidation pressure ($\sigma_{vo}' + \Delta \sigma' \geq \sigma_p'$) shown in Equation (2.11).

When $\sigma_{vo}' + \Delta \sigma' \leq \sigma_p'$;

$$\Delta e = C_r \log \frac{\sigma_{vo}' + \Delta \sigma'}{\sigma_{vo}'} \quad (2.10)$$

When $\sigma_{vo}' + \Delta \sigma' \geq \sigma_p'$;

$$\Delta e = C_r \log \frac{\sigma_p'}{\sigma_{vo}'} + C_c \log \frac{\sigma_{vo}' + \Delta \sigma'}{\sigma_p'} \quad (2.11)$$

The change in void ratio can be substituted into Equation (2.7) as described in Section 2.3.1 to allow the total consolidation settlement to be determined. In order to determine the consolidation settlement at a particular time throughout the consolidation process however, Terzaghi's one dimensional consolidation theory is utilised.

2.3.4 Terzaghi's One Dimensional Consolidation Theory

The theory to evaluate the rate of one dimensional consolidation was first proposed by Terzaghi (1925). Terzaghi's theory can be used to compute the time rate of volume change, settlements and pore pressure of the soil (Coduto 1998). Terzaghi implemented the following assumptions to develop his theory.

The assumptions of Terzaghi's Theory are:

1. Soil is homogenous - properties are considered consistent throughout;

2. Soil is fully saturated and solid particles and water are incompressible - no air is assumed to be present within the voids, and hence consolidation occurs due to the expulsion of pore water only;
3. Compression and flow are one dimensional (vertical) - no strains are present within the horizontal direction resulting in drainage only occurring in the vertical direction;
4. Strains are small - the coefficient of permeability (k) and the coefficient of volume compressibility (m_v) remain constant throughout the consolidation process;
5. Darcy's Law is valid at all hydraulic gradients - the permeability remains directly proportional to the flow rate throughout the soil media; and
6. No secondary consolidation (creep) occurs - the relationship between void ratio and effective stress is dependent upon the consolidation process.

Terzaghi developed the following differential equation using the previous assumptions.

$$\frac{\partial u}{\partial t} = c_v \frac{\partial^2 u}{\partial z^2} \quad (2.12)$$

where:

c_v = coefficient of consolidation

u = excess pore water pressure

z = depth below soil stratum

t = time

The coefficient of consolidation can be determined by Equation (2.13) when the coefficient of volume compressibility and vertical permeability is known, or can be found using graphical methods as described in Section 2.4, when applied to the settlement-time plots obtained from consolidation tests.

$$c_v = \frac{k_v}{\gamma_w m_v} \quad (2.13)$$

where:

γ_w = the unit weight of the water.

Terzaghi's differential equation for one dimensional consolidation can be considered as a diffusion equation for consolidation (Winterkorn and Fang 1990) and is similar to Fick's Law of Thermal Diffusion.

A mathematical solution can be obtained from Terzaghi's differential equation by applying appropriate boundary conditions, and using Fourier series to obtain a series solution. The generalised solution for the initial excess pore water pressure is evident in Equation (2.14).

$$\Delta u(z, t) = \Delta u_0 \sum_{m=0}^{m=\infty} \frac{2}{M} \sin(MZ) e^{-M^2 T} \quad (2.14)$$

where:

$$M = \frac{\pi}{2} (2m + 1) \quad (2.15)$$

$$Z = \frac{z}{H_{dr}} \quad (2.16)$$

$$T = \frac{t c_v}{H_{dr}^2} \quad (2.17)$$

In this series solution, both T and Z are dimensionless factors. The time factor (T) is dependent upon the coefficient of consolidation (c_v), the length of the drainage path (H_{dr}), and the duration of loading (t) where application of load is considered to be constant with time. The depth factor (Z) is dependent upon the length of the drainage path and the depth in consideration below the soil stratum (z), commonly defined as the centre of the clay layer if determining total consolidation settlement.

The length of the drainage path is measured as the longest length that drainage can occur in one dimension. If both boundaries (above and below) of the soil stratum are permeable, drainage is considered to be doubly drained and the drainage length is calculated as half of the total height of the clay layer ($H_{dr} = \frac{H}{2}$). If only one of these boundaries is permeable, the length of the drainage path is considered to be the total height of the clay layer ($H_{dr}=H$).

The length of the drainage path has a large effect on the rate of consolidation. When only one boundary is permeable, the time at which consolidation occurs is four times greater than that of two permeable boundaries, as time is proportional to the height of the layer squared ($t \propto H_{dr}^2$).

Modified Analytical Solution to Terzaghi's Differential Equation

Terzaghi's series solution described in Equation (2.14) has been modified by Lovisa et al. (2013) to incorporate a time factor (T^*) (Equation (2.18)) that is not dependent upon the length of the drainage path. This allows the U - T curve of a singly drained soil stratum and a doubly drained soil stratum to be individually graphed, allowing an easy comparison between the two to be made. The U - T curve of the singly and doubly drained solution can be seen in Figure 2.6.

As Terzaghi's classical solution considers a singly drained clay, the U - T curve obtained for this will align with the U - T curve obtained from the singly drained modified method (Mei and Chen 2013). The series solutions to a singly and doubly drained soil stratum, for a uniform initial excess pore water pressure are described in Equation (2.19) and (2.20) respectively. A derivation of the doubly drained solution can be seen in Appendix A.

$$T^* = \frac{c_v t}{D^2} \quad (2.18)$$

Doubly drained:

$$u(z, t) = \sum_{m=1}^{\infty} \left[\frac{2\Delta\sigma_v}{m\pi} (1 - (-1)^m \sin(\frac{n\pi z}{H})) \right] \exp(-m^2\pi^2 T^*) \quad (2.19)$$

Singly drained:

$$u(z, t) = \sum_{m=1}^{\infty} \frac{4\Delta\sigma_v}{(2m-1)\pi} \sin\left(\frac{(2m-1)\pi z}{2H}\right) \exp\left(\frac{-(2m-1)^2\pi^2 T^*}{4}\right) \quad (2.20)$$

where:

$\Delta\sigma_v$ = change in applied stress to the consolidating layer

Degree of Consolidation

The degree of consolidation is expressed as a percentage of excess pore water dissipated from the consolidating layer and represents conditions at a specific depth and time within the consolidating layer. The degree of consolidation is denoted by $U_z(t)$ and is determined via Equation (2.21).

$$U_z(t) = 1 - \sum_{m=0}^{\infty} \frac{2}{M} \sin(MZ) e^{-M^2 T} \quad (2.21)$$

The degree of consolidation can be determined from Figure 2.5 which uses isochrones for a given time factor throughout the depth of the compressible layer. The MATLAB code to produce this figure is shown in Appendix B-1.

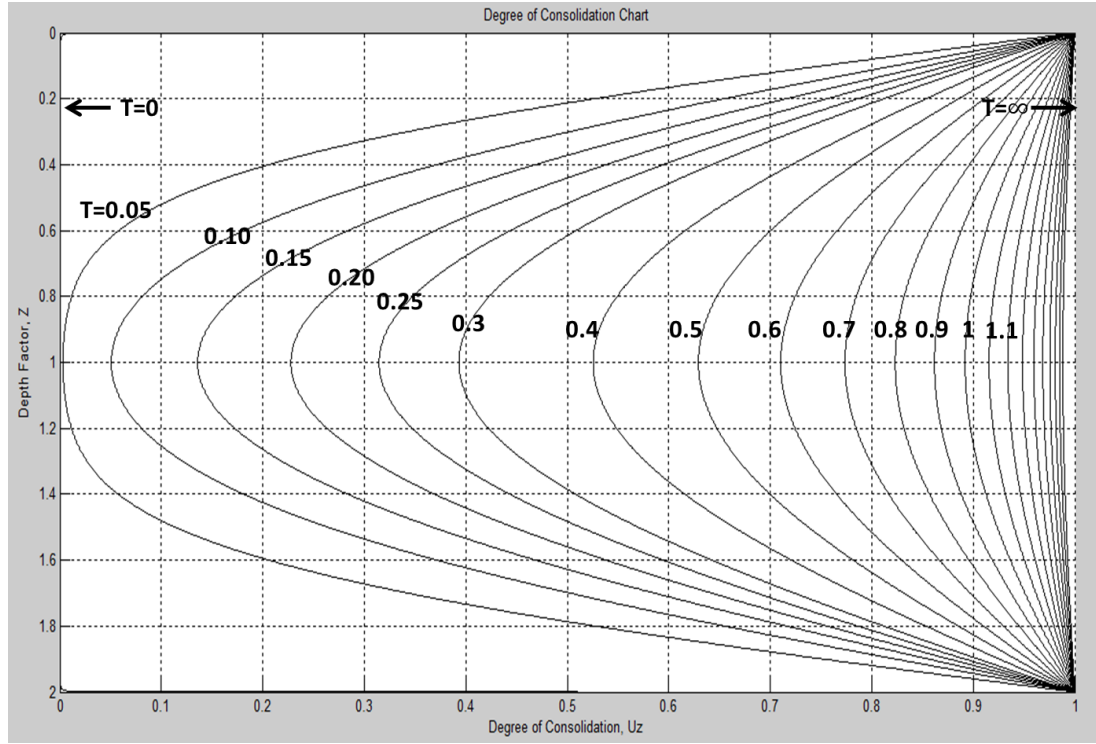


Figure 2.5: Degree of Consolidation Chart (U - Z - T Variation)

The degree of consolidation represents conditions specific to a depth and pressure. To determine a representative consolidation of the entire clay layer at time (t) after a stress is applied, average degree of consolidation theory is used.

Average Degree of Consolidation

The average degree of consolidation allows the percentage of consolidation at a specific time to be determined. It is a relation of the excess pore water that has been dissipated at this time due to the applied load, to the undissipated excess pore water. The average degree of consolidation is expressed in Equation (2.22).

$$U_{avg}(t) = 1 - \sum_{m=0}^{\infty} \frac{2}{M^2} e^{-M^2 T} \quad (2.22)$$

A graph that relates the time factor (T^*) to the average degree of consolidation, using Equations (2.19) and (2.20) for doubly drained and singly drained soil strata respectively, can be seen in Figure 2.6. MATLAB code to obtain these graphs is described in Appendix B-2. Equation (2.22) would allow a graph of the classical average degree of consolidation to be obtained, with the time factor of consolidation being dependent on the length of the drainage path (H_{dr}). This however, would align with the singly drained scenario, shown in Figure 2.6.

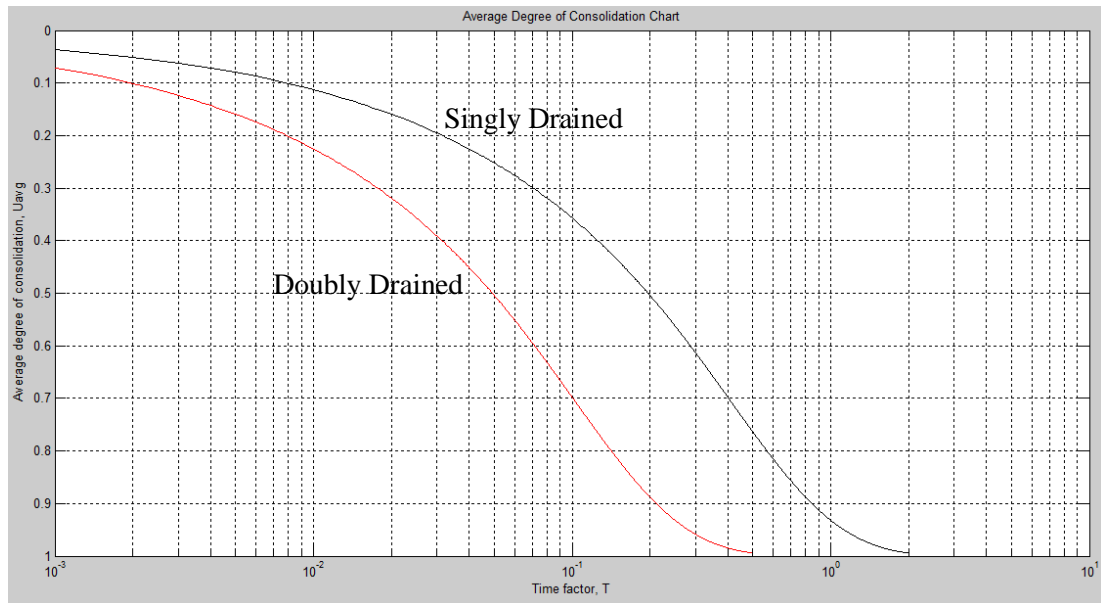


Figure 2.6: Average Degree of Consolidation Chart ($U - T$ chart)

The average degree of consolidation obtained from Figure 2.6 relies on a uniform distribution of excess pore water. As a uniform distribution does not always occur in reality, many investigations into this have been completed. Lovisa et al. (2010) considers various initial excess pore pressure distributions in one dimension in terms of average degree of consolidation. Average degree of consolidation curves ($U-T$ curves) for various non-uniform initial excess pore water distributions are presented in Lovisa and Sivakugan (2013).

The average degree of consolidation can also be calculated to incorporate linear and parabolic vertical strains though research conducted by Terzaghi and Frolich (1936) and Duncan (1993) with the average degree of consolidation time ($U-T$) curves with respect to three different vertical strain distributions, evident in Figure 2.7 (Janbu 1965).

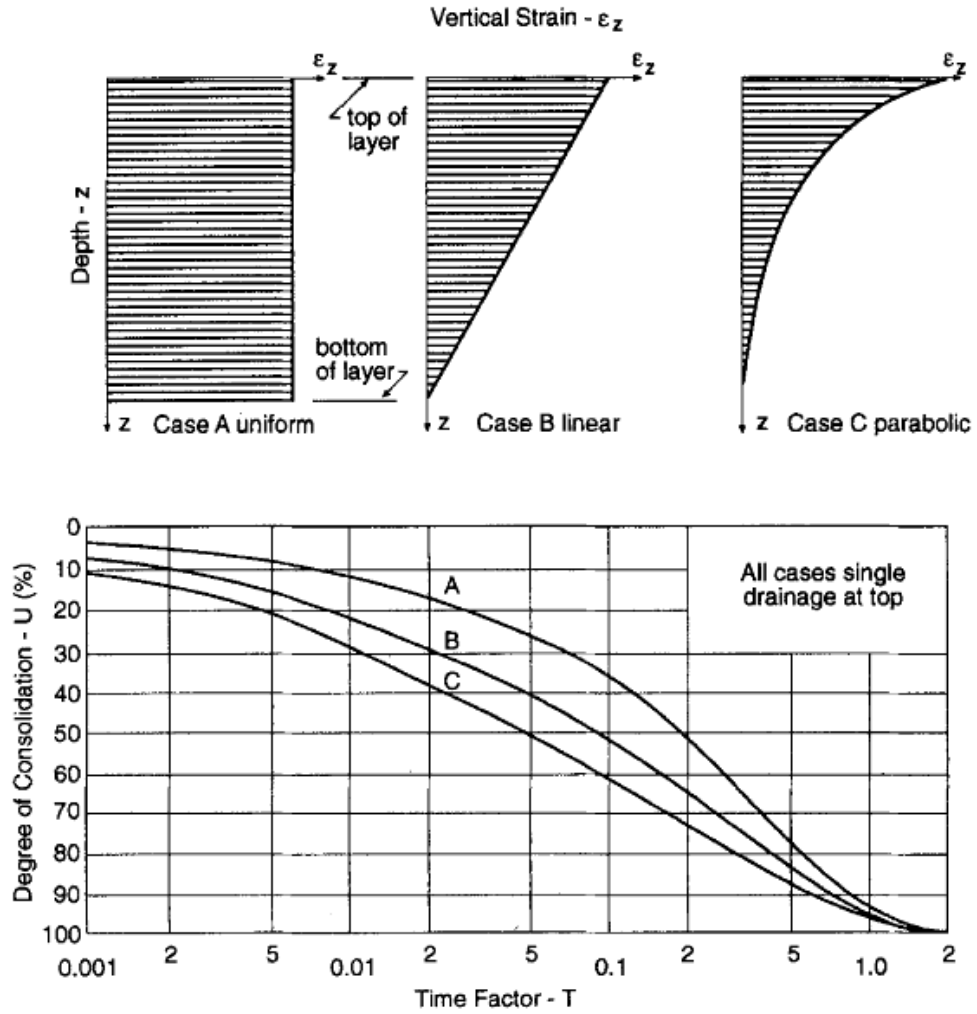


Figure 2.7: Influence of Strain Profile on Rate of Consolidation Settlement (Duncan 1993)

The average degree of consolidation is related to the total consolidation settlement ($s_{c,total}$) by Equation (2.23).

$$s_c = U_{avg} \times s_{c,total} \quad (2.23)$$

where $s_{c,total}$ is determined using Equation (2.7), as outlined in Section 2.3.1.

2.4 Calculating Coefficient of Consolidation (c_v)

The coefficient of consolidation (c_v) is determined using the settlement-time plot obtained in one dimensional consolidation testing for each load increment applied. Many methods have been developed to determine the coefficient of consolidation, with the most common being Casagrande's (1940) log time method and Taylor's (1948) square root of time method. These methods result in different values of c_v , with Taylor's method generally resulting in faster rates of consolidation (higher c_v values) (Duncan 1993).

Casagrande's Log Time Method

Casagrande's log time method is outlined in AS1289.6.6.1-1998 as a method to determine the coefficient of consolidation for primary consolidation (c_v) and also the coefficient of secondary compression (c_α) for secondary consolidation or creep. Figure 2.8 shows a typical consolidation settlement plot, where log time is in minutes and settlement is in millimetres (mm). This method relies on the determination of the 50 % primary consolidation in a doubly drained condition, which is related to the coefficient of consolidation by Equation (2.24).

$$c_v = \frac{0.049 H_{50}^2}{t_{50}} \quad (2.24)$$

where:

c_v = coefficient of consolidation, (m^2/yr)

H_{50} = thickness of the specimen,(mm), at 50 % consolidation of the loading increment

t_{50} = time for 50 % consolidation, (minutes)

To obtain the time for 50 % primary consolidation, the settlement resulting from 0 % and 100 % consolidation are first determined. The initial reading is designated the time (t_1) with the corresponding settlement reading (d_1). The time corresponding to the initial time multiplied by four ($4t_1$) is marked on the graph with its corresponding settlement reading (d_2). The settlement of 0 % consolidation can be determined by the difference between the settlement corresponding to $4t_1$ and the initial settlement reading (d_2-d_1), denoted y on Figure 2.8.

A tangent to the steepest part of the curve is drawn on the graph, as well as a tangent to the final points on the curve. At the intersection of these tangents, a horizontal line can be drawn, where it will extend to cross the curve. This point indicates 100 % consolidation.

Once the settlement corresponding to 0 and 100 % consolidation is established, the average of these settlements is obtained and marked on the curve and the corresponding time is determined as the time for 50 % primary consolidation (t_{50}).

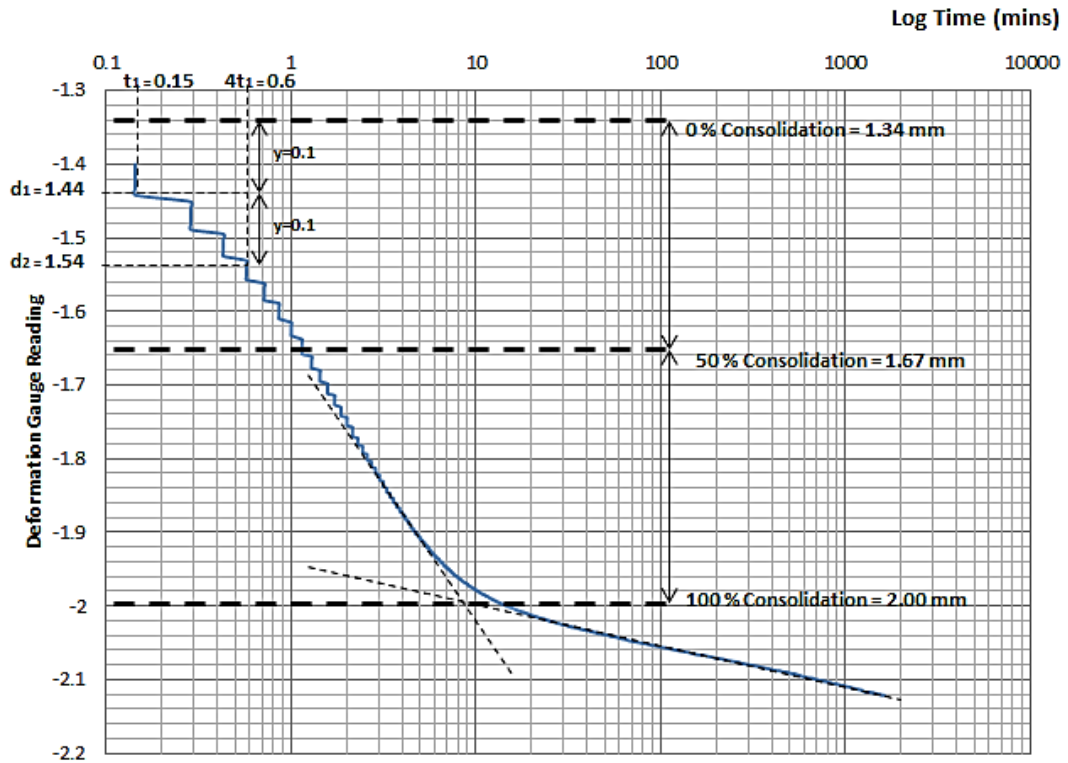


Figure 2.8: Casagrande's Log Time Method (using experimental results of 155 kPa loading increment)

Taylor's Square Root of Time method

Taylor's method is also presented as a method to calculate coefficient of consolidation (c_v) in AS1289.6.6.1-1998, where settlement (in mm) is plotted against the square root of time (in minutes).

The coefficient of consolidation is determined through Equation (2.25) which relates the time at 90 % consolidation to the average thickness of the consolidating layer for the doubly drained condition.

$$c_v = \frac{0.212 H_{90}^2}{t_{90}} \quad (2.25)$$

To quantify the time for 90 % consolidation, a straight line is drawn through 0 time and the initial portion of the curve, and the time at which the line finishes, denoted x . The time of $1.15x$ is marked on the plot at the same finishing length as the first line. A second line between the points of zero time and the $1.15x$ point is drawn, and the time at which it intersects the curve, determines the time for 90 % primary consolidation.

points to the curve in order to determine the coefficient of consolidation, compared to Taylor's and Casagrande's method which only fits one.

Numerous other methods have been derived to determine the coefficient of consolidation, many which include variations to overcome assumptions of Terzaghi's theory (Sridharan et al. 1987). One of these such methods is proposed by Lovisa et al. (2012) where non-uniform initial excess pore water pressure is taken into consideration when calculating the coefficient of consolidation.

2.5 Two and Three Dimensional Consolidation

Two dimensional consolidation consists of drainage and strains in both the vertical direction and one horizontal plane, occurring beneath a strip load, where a plane strain condition exists (Barnes 1995). Three dimensional radial consolidation is equivalent to two dimensional consolidation.

Consolidation in three dimensions takes into consideration drainage in the vertical direction and both horizontal planes. Three dimensional consolidation occurs beneath a circular, square or rectangular footing (Barnes 1995) or in a consolidating layer with a large depth compared to width and length.

It has been suggested by Davis and Poulos (1972) that the horizontal dissipation of pore pressure results in a rate of consolidation that is more rapid of which is not considered within one dimensional consolidation theory. Davis and Poulos (1972) also noted that three dimensional consolidation theory is not commonly used due to minimal theoretical practical solutions having been obtained for these.

2.5.1 Two and Three Dimensional Consolidation Theories

Two and three dimensional consolidation theories have been developed, with Terzaghi (1925) and Rendulic (1937) having proposed a two dimensional consolidation equation based upon the diffusion theory, and Biot (1941) proposing a general theory of three dimensional consolidation (Razouki and Al-Zayadi (2003); Poulos and Davis (1968)).

The Terzaghi-Rendulic equation for two dimensional consolidation is shown in Equation (2.26), as obtained from Razouki and Al-Zayadi (2003).

$$\frac{\partial u}{\partial t} = C_x \frac{\partial^2 u}{\partial x^2} + C_z \frac{\partial^2 u}{\partial z^2} + \frac{\partial u_e}{\partial t} \quad (2.26)$$

where:

C_x = horizontal coefficient of consolidation

C_z = vertical coefficient of consolidation

$\frac{\partial u_e}{\partial t}$ = rate of pore water pressure

u = excess pore water pressure

t = time after loading

A comparison has been made between the Terzaghi-Rendulic and Biot theories by Poulos and Davis (1968) and Murray (1978), and outlined in Razouki and Al-Zayadi (2003) where it is concluded that although Biot's theory allows the Mandel-Cryer effect to be taken into consideration where the diffusion theory does not, the diffusion theory of consolidation results in pore pressure estimates at the end of consolidation that can be deemed sufficiently accurate. The Mandel-Cryer effect describes the phenomena of pore pressure increasing in the centre of a consolidating region after the completion of load application, and before the dissipation of pore water ((Abousleiman et al. 1996); (Hwang et al. 1971)). This can only be seen in true consolidation theory such as Biot's. These results suggest that although Biot's method is a complete consolidation theory, the difficulty in using the method and the limited solutions to practical problems results in its minimal use.

Other differences between the methods arise from the calculation of the coefficient of consolidation. Rendulic's equations assume a single value of the coefficient of consolidation to be used in one, two and three dimensional consolidation calculations whereas Biot's theory identifies that this value depends on strain, resulting in the use of different coefficients of consolidation in each of these calculations (Murray 1978).

Terzaghi and Rendulic's equation of two dimensional consolidation can be considered a pseudo consolidation equation due to existing in an uncoupled form. Biot's theory can be considered a complete theory of consolidation due to its coupled form where both Darcy's law and mechanical deformation compatibility are taken into account (Davis and Poulos 1972).

Vertical Drains

Two dimensional consolidation has been considered by Barron (1948) with the use of sand (vertical) drains. Vertical drains are used in field situations to accelerate the rate of consolidation. This is completed by allowing pore water to dissipate at a faster rate in the horizontal direction by creating shorter horizontal drainage paths (Barnes 1995).

As the consolidation process of a vertical drain is dependent upon the coefficient of consolidation and the permeability in the horizontal and vertical directions, an equation was derived by Barron (1948) to quantify the degree of consolidation in the horizontal direction. Carrillo (1942) also quantified this process (Hong and Shang 1998).

Numerical Models

Numerical models for consolidation problems are often developed in order to quantify suitable parameters for use in determining the settlement properties of a consolidating layer. They allow coupled formulations such as Biot's theory to be implemented, such that solutions to consolidation problems can be determined without the difficulty of analytical methods.

Borges (2004) implemented a numerical model based on a finite element method, to determine the effect that vertical drains had on soft soils, to the rate of consolidation. A three dimensional analysis was completed with the use of Biot's consolidation theory, with results showing a large reduction in the total time of consolidation when compared to one dimensional theory.

A numerical prediction of large-strain consolidation was undertaken by Bartholomeeusen et al. (2002) where numerical models were implemented by various participants. All determined consolidation settlements were deemed to be accurate as a prediction of settlement in large strain situations; however the importance of initial parameters and assumptions was noted.

A finite nonlinear consolidation of a thick homogenous clay layer was considered by Gibson et al. (1981), with results showing an increased time rate of consolidation when compared to one dimensional consolidation theory. It was found however, that excess pore water pressure was underestimated when compared to one dimensional consolidation theory.

Many other numerical models have been developed, which overcome assumptions incorporated within Terzaghi's one dimensional consolidation theory. Due to the large quantity and broad range of available methods, only few were discussed.

2.6 Application – Land Reclamation

The determination of the rate of two and three dimensional consolidation has many field applications, including the application of land reclamation. Examples of this include the Port of Brisbane, Queensland, where land reclamation is currently being undertaken, and previous

land reclamation projects such as Bay Farm Island in San Francisco Bay and Kansai International Airport in Japan (Duncan 1993).

Land reclamation involves erecting permeable rock and sand seawalls in the direction of the ocean in order to acquire land. Fill material such as sands and gravels are generally used due to their drainage properties and are common to projects such as Bay Farm Island in San Francisco Bay and Kansai International Airport in Japan. This however results in an economically exorbitant cost as evident in Japan, where the cost of the fill alone for the artificial island of 4.3 km long, 1.3 km wide and 33 m thick and containing 184 million cubic meters of fill was 3.6 billion dollars (Duncan 1993).

The importance of two and three dimensional consolidation predictions to these applications arises when considering the underlying material of the acquired land. Bay farm Island was underlain by San Francisco Bay mud of 6 – 15 m, and Kansai International Airport underlain by approximately 20 m of soft alluvial clay followed by greater than 150 m of diluvial clay (Duncan 1993).

As outlined by Duncan (1993) in the *Twenty-Seventh Karl Terzaghi Lecture*, many problems arose with the determination of the magnitude and rate of consolidation settlement at these locations. One of the limitations identified was that of conventional consolidation theories in determining a suitable value of the coefficient of consolidation. The rate at which settlement occurred varied greatly dependent upon the coefficient of consolidation used, generally resulting in an over-prediction of the time rate of consolidation. The paper identified the benefit that would be obtained in using a two dimensional model to determine the rate of consolidation.

2.6.1 Port of Brisbane, Queensland, Australia

The Port of Brisbane land reclamation project involves the acquisition of approximately 235 hectares of additional land by implementing a 4.6 km long rock and sand seawall as the perimeter of the containment area (Ganesalingam et al. 2012b). The area is further segregated by containment bunds, where fill material is then placed (see Figure 2.10).



Figure 2.10: Aerial view of Land Reclamation at the Port of Brisbane (Ganesalingam et al. 2012a)

As previously identified, filling these containment bunds with a material such as sand would incur an economically exorbitant cost and hence, the contained bunds are filled with dredged materials, not only providing a cheaper alternative, but creating an environmentally friendly means of disposing of dredged materials (Ganesalingam et al. 2012b). As both the dredged materials and Holocene clay layer underlying the containment bunds have poor drainage properties and compressibility (Ganesalingam et al. 2012a), the process of consolidation can be timely.

In order to accelerate consolidation, ground improvement techniques are used such as vertical drains and preloading with sand when a suitable bearing capacity has been achieved. Due to the simultaneous drainage that occurs by the vertical drains and the permeable containment bunds, a three dimensional consolidation process arises.

The Port of Brisbane currently uses numerical software called CAOS (Consolidation Analysis of Soils) that uses past consolidation settlement rates to determine future rates. Limitations in consolidation theory results in the difficulty of the estimation of the rate of settlement, with one dimensional consolidation theory possibly overestimating the time taken for consolidation to be achieved. This highlights the importance and necessity of the time rate of three dimensional consolidation.

Chapter 3: Analytical Solution of Three Dimensional Consolidation

3.1 General

An analytical solution for axisymmetric three dimensional consolidation was derived through the extension of the one dimensional differential equation developed by Terzaghi (1925). The three dimensional analytical solution applies to peripheral drainage and vertical drainage through the top and bottom boundaries of the sample. The solution is a function of both the horizontal and vertical coefficient of consolidation and the radius and height of the sample. Through the use of MATLAB, the method of nonlinear least squares was used to extend the solution to various radius/height (R/H) ratios. This chapter presents the three dimensional analytical solution, as derived and presented in the paper by Lovisa et al. (2014).

3.2 Extension from One Dimension to Three Dimensions

The rate of one dimensional consolidation was first proposed by Terzaghi (1925), with the following differential equation (Equation (3.1)), as previously discussed in Section 2.3.4.

$$\frac{\partial u}{\partial t} = c_v \frac{\partial^2 u}{\partial z^2} \quad (3.1)$$

Many assumptions were made in the development of this differential equation, the most prominent to this thesis being that strains and drainage were only considered in the vertical direction.

The one dimensional differential equation was extended to an axisymmetric three dimensional differential equation through the incorporation of the radial component (r) and the horizontal coefficient of consolidation (c_h). This was completed in order to consider the addition of peripheral drainage to the sample. The governing equation for axisymmetric three dimensional consolidation is evident in Equation (3.2).

$$\frac{\partial u}{\partial t} = c_v \frac{\partial^2 u}{\partial z^2} + c_h \left[\frac{\partial^2 u}{\partial r^2} + \frac{1}{r} \frac{\partial u}{\partial r} \right] \quad (3.2)$$

where $0 \leq r \leq R$, $0 \leq z \leq H$ and $0 \leq t \leq \infty$

To solve this partial differential equation, scaled variables with respect to r , z , t and u were introduced. These are evident in Equations (3.3), (3.4) and (3.5) respectively.

$$r = \beta X \quad (3.3)$$

$$z = \gamma Z \quad (3.4)$$

$$t = \tau T \quad (3.5)$$

By solving the partial differential equation with these scaled variables, Equation (3.2) results, with the corresponding limits presented following.

$$\frac{\gamma^2}{c_v \tau} \frac{\partial u}{\partial t} = \frac{\partial^2 u}{\partial Z^2} + \frac{c_h \gamma^2}{c_v \beta^2} \left[\frac{\partial^2 u}{\partial X^2} + \frac{1}{X} \frac{\partial u}{\partial X} \right] \quad (3.6)$$

where:

$$0 \leq X \leq \sqrt{\frac{c_v}{c_h}} \frac{R}{H}$$

$$0 \leq Z \leq H$$

$$0 \leq T \leq \infty$$

The series solution of this partial differential equation, as evident in Equation (3.7) can be determined by assuming a symmetric problem with $u = 0$ at $r = R_0$ and $z = 0, D$.

$$u(z, r, t) = \sum_{m=1}^M \sum_{n=1}^N A_{mn} \sin\left(\frac{m\pi z}{D}\right) J_0\left(\frac{\lambda_n r}{R_0}\right) \exp\left(-\left(\left(\frac{m\pi z}{D}\right)^2 + \left(\frac{\lambda_n r}{R_0}\right)^2\right) c_v t\right) \quad (3.7)$$

The Bessel function (J_0) is of the first kind of zero order, where λ_n are the zeroes of this function. This is represented by Equation (3.8).

$$r^2 \frac{d^2 R}{dr^2} + r \frac{dR}{dr} + r^2 R = 0 \quad (3.8)$$

Using the series solution evident in Equation (3.7) the average degree of consolidation curves (U - T curves) were developed for various R/H values. The resulting U - T curves are evident in Figure 3.1.

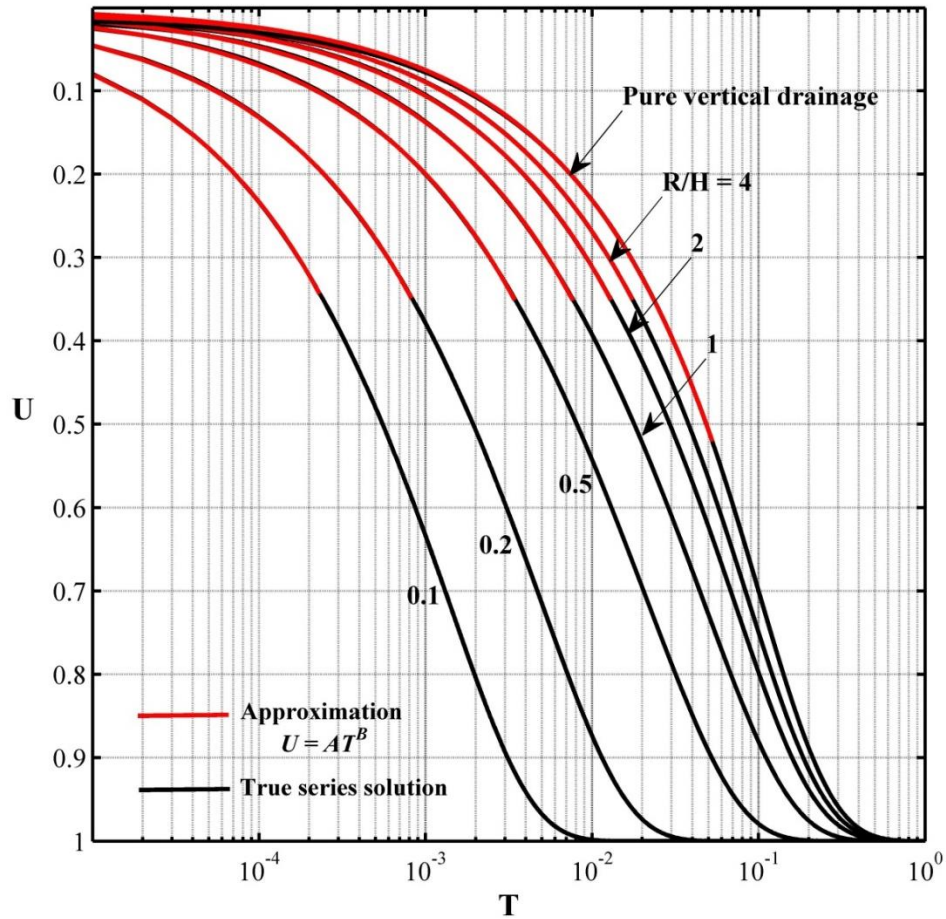


Figure 3.1: Average Degree of Consolidation Curves for Varying R/H Ratios (Lovisa et al. 2014)

An R/H value of 320 was used in Figure 3.1 to represent pure vertical drainage. This indicates a radius much larger than the height of the sample analysed. This correlates to general one dimensional consolidation assumptions. As the R/H value is decreased, a faster rate is observed. This correlates to a larger height value than radius, and indicates increased horizontal drainage.

To quantify the rate of horizontal drainage, the time factor at 50 % consolidation and 90 % consolidation for Casagrande's and Taylor's method respectively was obtained. Table 3.1 describes the expected time factor values of Casagrande's and Taylor's method for a variety of R/H values, and the domain to which they apply.

The domain was determined for the various $U-T$ curves through approximations of regions of these curves. Approximations for each region were inputted into MATLAB where constants were assumed, and the method of nonlinear least squares was used to determine the error

associated with these (Lovisa et al. 2012). Iteration was continued until an error value less than 1.0×10^{-3} was obtained (Lovisa et al. 2012).

Table 3.1: Modified curve-fitting parameters (Lovisa et al. 2014)

$R/H \times (C_h/C_v)^{0.5}$	Domain	Casagrande		Taylor		
		f_c	T_{50}	f_T	B	T_{90}
∞	52.1	4	0.049	1.15	0.5	0.212
320	52.1	4.15	0.048	1.14	0.49	0.212
7	32	4.23	0.0424	1.17	0.48	0.1968
4	32	4.27	0.037	1.21	0.48	0.185
3	29	4.29	0.034	1.24	0.47	0.176
2	27	4.33	0.029	1.29	0.47	0.158
1.5	27	4.38	0.0247	1.32	0.47	0.1418
1	27	4.4	0.017	1.38	0.47	0.11
0.8	27	4.4	0.0143	1.4	0.47	0.0915
0.6	27	4.4	0.0103	1.41	0.47	0.0666
0.5	27	4.38	0.008	1.43	0.47	0.052
0.4	27	4.43	0.0059	1.39	0.47	0.0376
0.3	27	4.42	0.0038	1.37	0.47	0.0235
0.2	27	4.41	0.0019	1.34	0.47	0.0115
0.1	27	4.4	0.00055	1.3	0.47	0.003

By applying these modified curve fitting parameters to the corresponding settlement-time plot, the coefficient of consolidation can be determined using the known graphical process of Casagrande's or Taylor's method.

Furthermore, the relationship between the time factor and the radial factor ($R/H \times (C_h/C_v)^{0.5}$) can be graphed, as evident in Figure 3.2 and Figure 3.3 for Casagrande's and Taylor's method respectively. By utilising these figures, the anisotropy of the sample can be quantified. An example of this, using results obtained experimentally, is evident in Section 5.5.

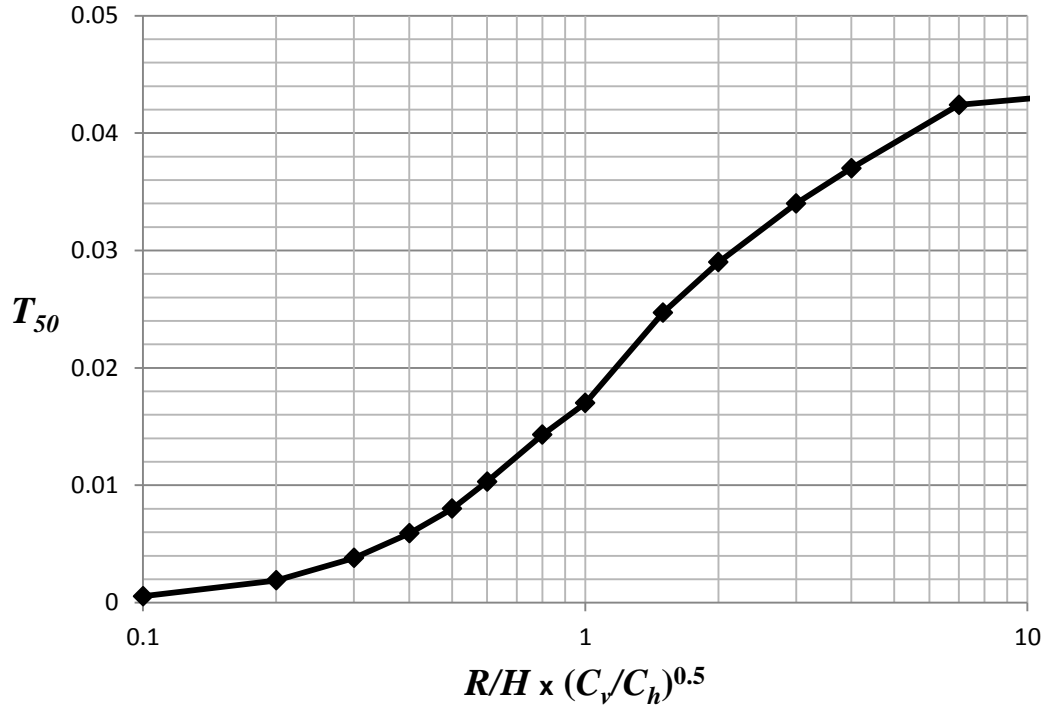


Figure 3.2: Quantifying Anisotropy using Modified Time Factors – Casagrande’s Method (Lovisa et al. 2014)

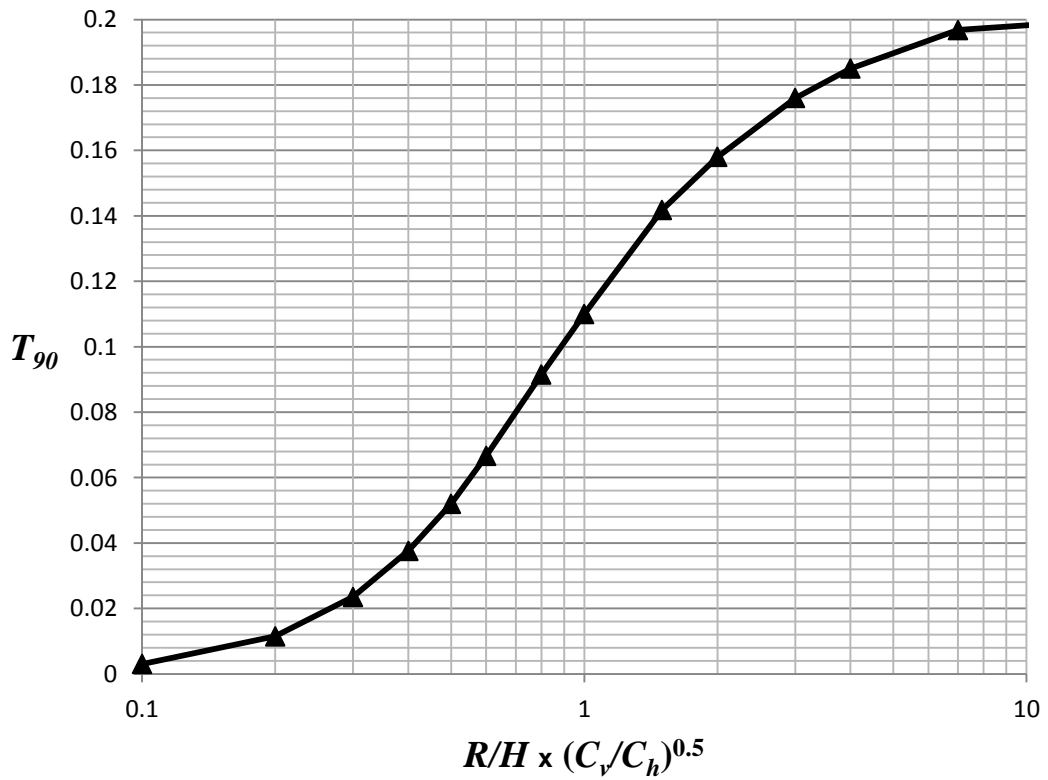


Figure 3.3: Quantifying Anisotropy using Modified Time Factors – Taylor’s Method (Lovisa et al. 2014)

3.3 Summary

The analytical solution of three dimensional consolidation was presented in this chapter. By extending Terzaghi's one dimensional consolidation theory, a partial differential equation was determined for a three dimensional consolidation scenario, accounting for vertical two way drainage and peripheral drainage. The analytical solution obtained from this partial differential equation allowed the $U-T$ graph of various R/H values to be determined.

Through the use of a MATLAB code, modified curve fitting parameters were derived to account for these various R/H values. The time factor at 50 % or 90 % for Casagrande's and Taylor's method respectively was plotted against a radial factor, allowing the horizontal coefficient of consolidation to be quantified when a time factor value is known.

Chapter 4: Experimental Investigation Methodology

4.1 Overview

The primary objective of this thesis was to quantify the rate of consolidation when drainage in both the vertical and radial direction (axisymmetric three dimensional consolidation) was considered, in comparison to the time rate of consolidation considering vertical drainage only (one dimensional consolidation).

In order to achieve this objective, extensive laboratory investigation was completed. This investigation was completed on kaolin clay, with properties evident in Section 4.2.1. Experimental investigation comprised standard one dimensional consolidation tests, three dimensional axisymmetric consolidation tests using a new apparatus and permeability testing on horizontally and vertically cut samples, allowing direct measurement of permeability to be acquired.

In this chapter, the experimental investigations undertaken will be described. A discussion of the results obtained will be discussed in following Sections.

4.2 Soil Properties

The experiments were conducted on kaolin clay, and included a range of one dimensional and three dimensional consolidation tests. The kaolin clay used exhibited the properties evident in Table 4.1.

Table 4.1: Properties of Kaolin Clay

Specific Gravity (G_s) (g/cm^3)	2.47
Plastic Limit (PL) (%)	37.2
Liquid Limit (LL) (%)	81.4
Linear Shrinkage (LS) (%)	12
Plasticity Index (PI) (%)	44.2

4.2.1 Determination of Soil Parameters

To determine soil parameters for data analysis, the following soil classification tests evident in Table 4.2 were undertaken.

Table 4.2: Tests undertaken for Soil Classification

Test	Standard	Parameter Obtained
Determination of the soil particle density of a soil – Standard Method	AS1289.3.5.1-2006	Soil particle density of Kaolin (ρ_s)

Determination of the plastic limit of a soil – Standard Method	AS1289.3.2.1-2009	Plastic Limit (PL)
Determination of the cone liquid limit of a soil	AS1289.3.9.1-2002	Liquid Limit (LL)
Determination of linear shrinkage of a soil	AS1289.3.4.1-2008	Linear Shrinkage (LS)

4.3 Tall Oedometer for Sample Preparation

An artificial soil sample was prepared using kaolin clay in a dry powdered form, mixed with water to form slurry. Two batches of slurry were prepared throughout the duration of the laboratory investigation, the first with a water content of 148 % and the second with a water content of 101 %. The first slurry was used for all standard one dimensional consolidation and three dimensional consolidation tests, whereas the second water content was used to determine horizontal permeability (k_h). A second slurry was required in order to ensure a larger final sample was achieved.

To prepare the slurry for use within a one or three dimensional consolidation apparatus, a tall oedometer was used, with apparatus depicted in Figure 4.1. This method relied on the consolidation of the sample by application of increasing hydraulic pressure with time.

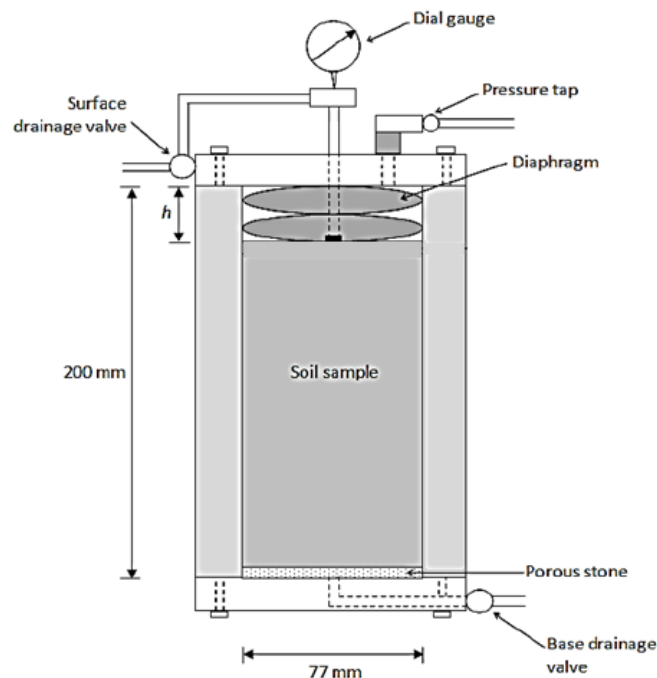


Figure 4.1: Tall Oedometer Schematic (Lovisa and Sivakugan)

The slurry was placed in the tall oedometer, with a porous stone below the sample allowing single drainage from the bottom of the apparatus. A low hydraulic pressure of 20 kPa was applied, and the sample was left to consolidate for approximately 24 hours, or until it achieved very little consolidation at the applied pressure. The pressure was increased in increments of double the current load, until the diaphragm became too extended at which point the apparatus was disassembled and an additional spacer stone placed on top of the sample. The diaphragm was reassembled and pressure further increased in increments to 160 kPa.

Throughout the number of experiments, the final height of the sample ranged between 5 cm and 7 cm, with a corresponding moisture content between 60 to 68 %. At this stage, the sample was extruded for use within the consolidation apparatus. The tall oedometer procedure for slurry preparation is further described in Appendix C.

4.4 Homogeneity between samples

To ensure homogeneity of the range of laboratory investigations, a range of monitoring techniques were undertaken.

The kaolin slurry remained the same for the extent of the standard (horizontal cut) samples, to minimise the variance in results from mixing new batches throughout the investigations. The kaolin slurry used for the vertically cut sample (to complete horizontal permeability tests), differed to the other tests undertaken, however this was necessary to ensure the height of the final sample would be suffice to cut a sample.

The final water contents at extrusion of the tall oedometer were monitored throughout testing to ensure that the water content remained within comparable limits. The load schedule was kept throughout the testing process, with all samples being placed under the same loading increments.

4.5 One Dimensional Consolidation

Standard one dimensional consolidation tests were completed to *AS1289.6.6.1-1998: Soil strength and consolidation tests-Determination of the one-dimensional consolidation properties of a soil-Standard Method*, using the procedure outlined in Section 2.3.2. One dimensional settlement-time plots were used to determine the vertical coefficient of consolidation (c_v) through the use of both Casagrande's and Taylor's graphical method.

Two one dimensional consolidation tests were completed on a sample of 63 mm diameter with loading increments from 1 kPa to 2500 kPa. The 63 mm diameter consolidation ring

was used, due to the diameter of the tall oedometer being 77 mm. This additional clearance allowed minimal edge disturbance to be included within the sample. Settlement-time plots were obtained for these samples, which were used to determine the vertical coefficient of consolidation using both Taylor's and Casagrande's graphical methods.

As the coefficient of consolidation is directly proportional to permeability of a sample (see Equation (2.13)), permeability was measured in conjunction with consolidation testing, through the use of a standard rowe cell of 75 mm diameter with permeability capabilities. Two horizontally cut samples to determine permeability in the vertical direction (k_v), denoted by (a) in Figure 4.2 and two vertically cut samples, denoted by (b) in Figure 4.2 to determine permeability in the horizontal direction (k_h), were completed. This allowed the permeability anisotropy to be quantified.

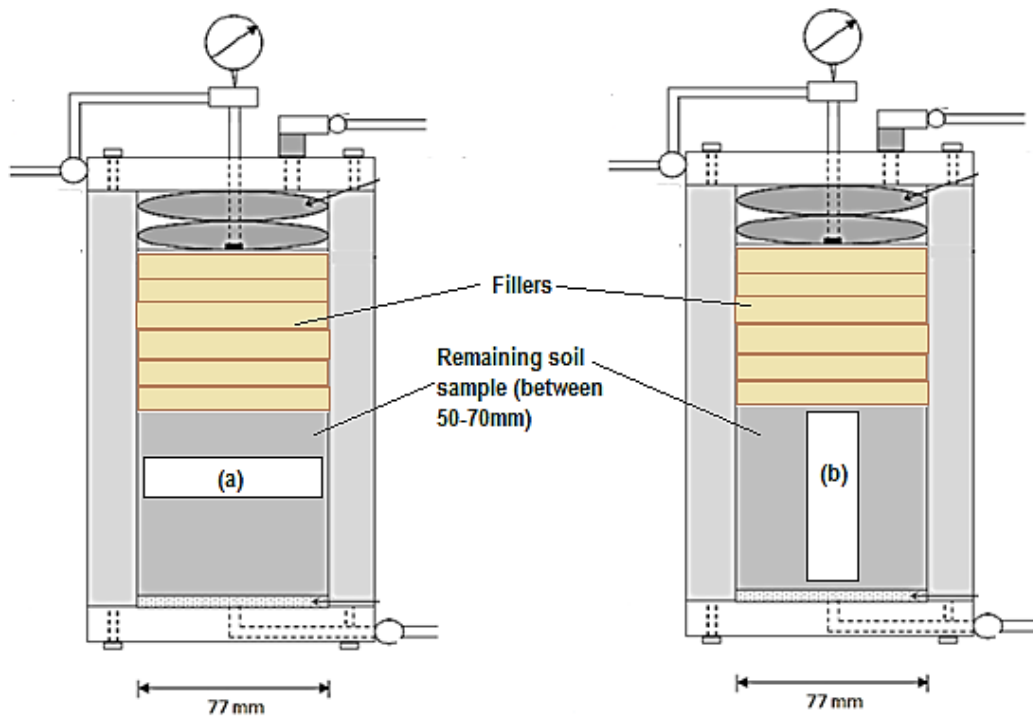


Figure 4.2: Orientation of Permeability Consolidation Samples

4.6 Three Dimensional Consolidation

A new apparatus for three dimensional axisymmetric consolidation was used to obtain settlement-time plots of a three dimensional scenario. A stainless steel consolidation cell with a height of 63 mm and diameter of 63 mm (height/diameter ratio of 1) was used in the standard consolidation apparatus, following the same procedure as one dimensional consolidation. These dimensions were selected to maximise the sample height, thereby maximising the three dimensional effects of consolidation. This can be seen in the analytical

solution, depicted in Figure 3.1 where, as R/H decreases, the rate of consolidation and effects of anisotropy increase. As the maximum height that could fit within the standard oedometer was 63mm, this was the height and diameter chosen.

The consolidation cell was porous at the top and bottom of the sample by utilising porous stones and peripherally through the use of a porous fabric. This allowed both vertical and peripheral drainage of the sample, resulting in a three dimensional axisymmetric consolidation scenario. The schematic of the consolidation can be seen in Figure 4.3.

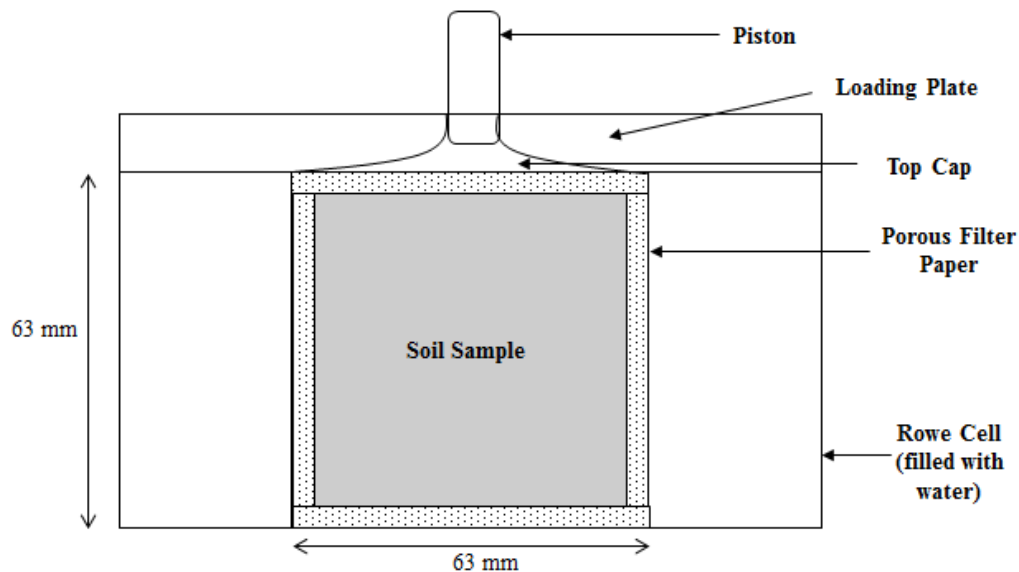


Figure 4.3: Three Dimensional Consolidation Apparatus Schematic

4.7 Scanning Electron Microscope (SEM)

A Scanning Electron Microscope (SEM) was used to produce a high spatial resolution microscopic image of the clay particles within a sample, allowing the orientation, shape composition and void size of the sample to be analysed (Todokoro and Ezumi 1999).

SEM images were obtained through the Advanced Analytical Centre, located at James Cook University, in order to view the particle orientation at stages throughout the preparation and consolidation of the samples. A SEM image was obtained after sample preparation (after the tall oedometer), after a one dimensional consolidation test that had undergone both loading and unloading, and at the completion of a three dimensional consolidation test that had undergone loading only. Images obtained from the SEM are evident in Section 5.7.

4.8 Summary

The methodology of experimental investigation was discussed in this chapter. A variety of one and three dimensional consolidation tests were undertaken in order to achieve the aims of this study. SEM scanning was completed on a representative number of samples in order to view the particle orientation at a microscopic level. Discussions of the results obtained through this methodology are evident in the following chapters.

Chapter 5: Quantifying the Horizontal Coefficient of Consolidation (c_h)

5.1 General

The horizontal coefficient of consolidation (c_h) is a property of the soil in the horizontal direction. Through the use of an equivalent coefficient of three dimensional consolidation ($c_{3D,equiv}$), the time factor of consolidation at 50 % and 90 % consolidation can be determined for Casagrande's and Taylor's method respectively. These values can be used in conjunction with Figure 3.2 and Figure 3.3 to calculate the anisotropy of the soil, therefore determining the horizontal coefficient of consolidation. This chapter presents the process involved in determining the horizontal coefficient of consolidation (c_h).

5.2 Experimental Results of Coefficient of Consolidation (c_v) from One Dimensional Settlement-time plots

The vertical coefficient of consolidation was determined using Casagrande's and Taylor's graphical methods for one dimensional settlement-time plots, as detailed in Section 2.4. The results obtained through laboratory investigation showed that the coefficient of consolidation between these methods varied significantly, with Taylor's method estimating a greater coefficient of up to 4.66 times that of Casagrande's method. An example of this is evident in Figure 5.1, with the difference between the obtained values of Taylor's and Casagrande's method of a one dimensional sample presented. The entirety of these values is presented in Appendix D-1.

Taylor's method often results in a greater rate of consolidation than that obtained by Casagrande's method, as noted by Lovisa and Sivakugan (2013). Taylor's method could not be completed in some circumstances however, as the starting settlement point could not be passed through the initial region of the curve. This is further explained following, when utilising Taylor's method for three dimensional settlement-time plots.

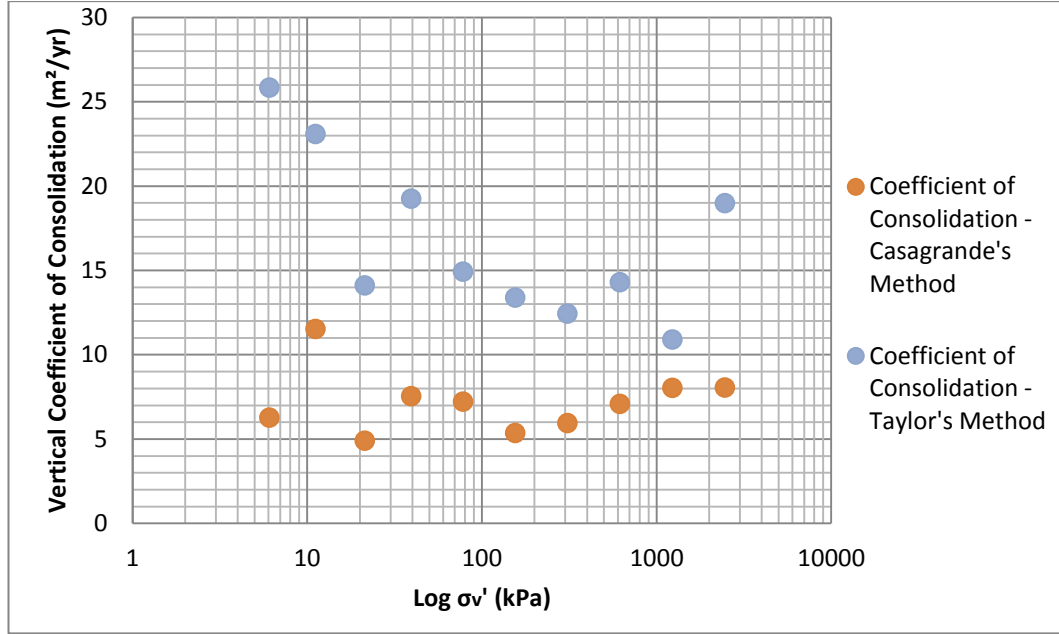


Figure 5.1: Vertical Coefficient of Consolidation - Comparison between Casagrande's and Taylor's Graphical Method

5.3 Coefficient of Equivalent Three Dimensional Consolidation ($c_{3Dequiv}$)

An equivalent three dimensional coefficient of consolidation was determined for both Taylor's and Casagrande's method using the three dimensional consolidation settlement-time plots. The equivalent three dimensional coefficient of consolidation was achieved using Equation (5.1) and Equation (5.2) , for Taylor's and Casagrande's methods respectively, reliant upon the time factor of one dimensional consolidation, and the height and time of the three dimensional sample.

$$c_{v,3Dequiv} = \frac{T_{50,1D}H^2}{t_{50,3D}^2} \quad (5.1)$$

$$c_{v,3Dequiv} = \frac{T_{90,1D}H^2}{t_{90,3D}^2} \quad (5.2)$$

The equivalent three dimensional coefficient of consolidation was determined for the modified three dimensional consolidation, and the standard one dimensional method for both Taylor's and Casagrande's method.

5.3.1 Modified Taylor's and Casagrande's Method

Modifications of Taylor's and Casagrande's methods for varying R/H ratios were presented in Section 3.2 and are summarised in Table 5.1. From this table, it is evident that the domain greatly decreases when applying Taylor's and Casagrande's method to three dimensional consolidation settlement-time plots.

Table 5.1: Corrections of Taylor's and Casagrande's Method to Three Dimensional Consolidation Settlement-time plots

R/H	c_h/c_v	Domain	Casagrande's Method		Taylor's Method		
			f_c	T_{50}	f_T	B	T_{90}
100000000	0	52.1	4	0.049	1.15	0.5	0.212
0.5	4	23	4.38	0.008	1.43	0.47	0.052

Taylor's Method

Although both methods were completed on the three dimensional settlement-time plots, it became evident that Taylor's method was unable to be used for many of the early loading increments, for both the corrected and uncorrected methods. This was due to the difference in the initial height of the sample, compared to the rate of which the sample was consolidating. This resulted in the inability to draw a tangent connecting the initial height with the initial portion of the curve.

Further difficulty was encountered when completing Taylor's method on the corrected settlement-time plots due to the reduced domain. The reduced domain resulted in further subjectivity of drawing a tangent connecting the initial dial gauge reading and portion of the curve, due to the little region that it applied to.

Although all data was attained for Taylor's method, Casagrande's method was favoured throughout this thesis due to a greater reliability in obtaining a coefficient of consolidation for a majority of the loading increments.

Casagrande's Method

When applying the corrected Casagrande factor (f_c) value to the three dimensional settlement-time plots, the equivalent coefficient of consolidation values varied up to 65 % when compared to the unmodified method. Figure 5.2 shows a representative sample of the coefficient of consolidation values of a three dimensional sample. In this figure, the corrected values use a f_c of 4.38 and a domain up to 30 %.

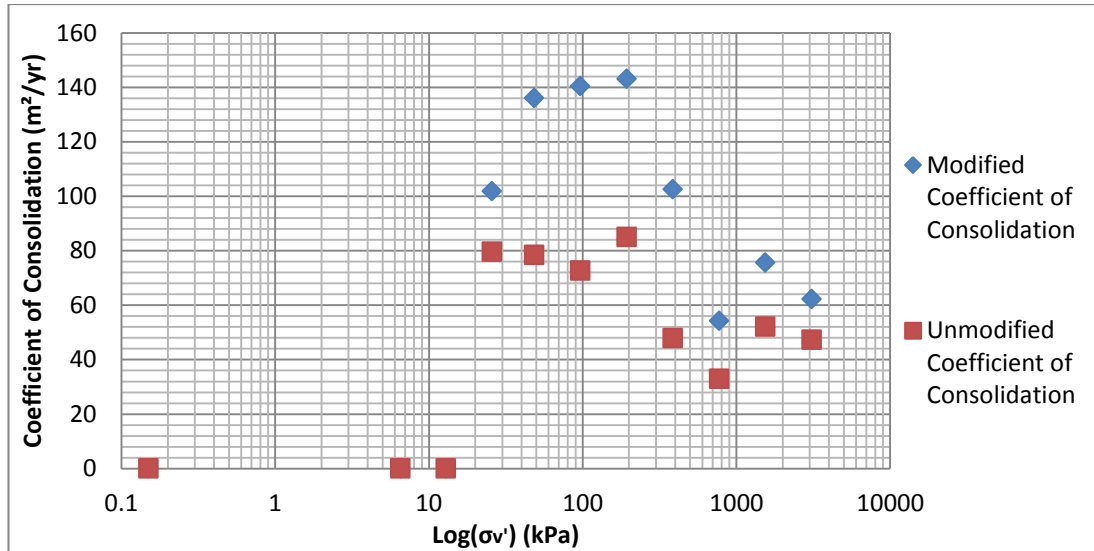


Figure 5.2: Modified vs. Non-Modified Coefficient of Consolidation Values for a Three Dimensional Sample

It is evident from Figure 5.2 that the modified method has a significant effect on the equivalent rate of consolidation. When completing the corrected Casagrande's graphical method, it was noted that the initial dial gauge reading often had to be chosen for d_0 . This was due to the decreased domain, and the larger f_c multiplication factor. If a larger d_0 was chosen, d_1 would often not fall within the 30 % domain.

5.4 Time Factor of Three Dimensional Consolidation ($T_{50,3D}$)

The time factor of three dimensional consolidation ($T_{50,3D}$) was acquired by using the equivalent rate of three dimensional consolidation ($c_{3Dequiv}$).

As the coefficient of consolidation is a property of the soil that is independent of the drainage conditions, the one dimensional coefficient of consolidation should be the same as the vertical coefficient of consolidation obtained for three dimensional consolidation tests.

The time factor however will vary, as the time to reach 50 % consolidation (t_{50}) or 90 % consolidation (t_{90}) for Casagrande's and Taylor's method respectively, differs according to the drainage conditions of the soil sample. Using this information, the three dimensional time factor ($T_{50,3D}$) was determined.

Casagrande's Method

The one dimensional time factor of Casagrande's method (T_{50}) of 0.049 relies on the time (t_{50}) and height (H) at 50 % consolidation. This relationship can be seen in Equation (5.3),

where, for explanation purposes, the parameters are referred to using one dimensional subscripts.

$$T_{50,1D} = \frac{c_v t_{50,1D}}{H^2} \quad (5.3)$$

The same methodology can be applied to the time factor at 50 % of three dimensional consolidation, represented by Equation (5.4).

$$T_{50,3D} = \frac{c_v t_{50,3D}}{H^2} \quad (5.4)$$

As the coefficient of one dimensional consolidation (c_v) is the same as the vertical coefficient of three dimensional consolidation, the time factor of three dimensional consolidation can be determined through the use of an equivalent rate of three dimensional consolidation ($c_{3Dequiv}$).

This is achieved by applying the modified one dimensional Casagrande's curve fitting method to three dimensional settlement-time plots. The equivalent rate of three dimensional consolidation relies on the one dimensional time factor of 0.049, however will use the height and time at 50 % consolidation from the three dimensional settlement-time plot. This relationship can be seen in Equation (5.5).

$$T_{50,3D} = \frac{c_{3D\ equiv} t_{50,3D}}{H^2} \quad (5.5)$$

When dividing Equation (5.5) by Equation (5.4), Equation (5.6) results.

$$\frac{T_{50,3D}}{T_{50,1D}} = \frac{c_v}{c_{3D,equiv}} \quad (5.6)$$

As the time factor of one dimensional consolidation is known to be 0.049 and the equivalent coefficient of three dimensional consolidation and one dimensional consolidation can be obtained using the settlement-time plot for one and three dimensional consolidation tests respectively, the time factor at 50 % consolidation for a three dimensional sample can be determined.

Taylor's Method

A similar procedure is used to determine the time factor of three dimensional consolidation for Taylor's method. The time factor however, is at 90 % consolidation (T_{90}), with the

respective time (t_{90}) of the sample and height (H) of the sample at 90 % consolidation. This relationship can be seen in Equation (5.7).

$$T_{90,1D} = \frac{c_v t_{90,1D}}{H^2} \quad (5.7)$$

As per Casagrande's method, the time factor of three dimensional consolidation can be determined using an equivalent rate of three dimensional consolidation, expressed in Equation (5.8).

$$\frac{T_{90,3D}}{T_{90,1D}} = \frac{c_v}{c_{3Dequiv}} \quad (5.8)$$

The time factor for one dimensional consolidation using Taylor's method is 0.212, as shown in Section 2.4. Again, the coefficient of consolidation for both one dimensional consolidation and the equivalent three dimensional consolidation can be determined through the settlement-time plots of one and three dimensional tests respectively, resulting in the only unknown variable being the time factor at 90 % consolidation.

5.4.1 Finding $T_{50,3D}$ – An example using Casagrande's Method

In order to further explain the procedure for determining the time factor of three dimensional consolidation, the following example is provided. This example uses Casagrande's method, allowing the time factor of three dimensional consolidation at 50 % to be determined. Once this method is understood, the theory can be easily applied to Taylor's method.

The rate of one dimensional consolidation at an applied load of 155 kPa is determined using the standard Casagrande's method resulting in a one dimensional coefficient of consolidation of 8.12 m²/yr. The settlement-time plot obtained for the same loading increment of the axisymmetric three dimensional consolidation apparatus at an applied load of 193 kPa is analysed to determine $c_{3D,equiv}$.

By applying the modified Casagrande's method to the axisymmetric three dimensional consolidation settlement-time plot, the resulting settlement (d_{50}) at 50 % consolidation is 4.195 mm, with a corresponding time of 2.0 minutes. The initial height of the three dimensional sample was 63 mm. This information is used to determine the equivalent rate of three dimensional consolidation, evident in Equation (5.9).

$$\begin{aligned}
c_{v,3D \text{ equiv}} &= \frac{T_{50,1D} H_{50}^2}{t_{50,3D}} & (5.9) \\
&= \frac{0.049 \times (63.00 \text{ mm} - 4.195 \text{ mm})^2}{2.0 \text{ min}} \times \frac{60 \text{ min}}{\text{hr}} \times \frac{24 \text{ hrs}}{\text{day}} \times \frac{365 \text{ days}}{\text{year}} \times \frac{1 \text{ m}^2}{1000^2 \text{ mm}^2} \\
&= 44.530 \frac{\text{m}^2}{\text{yr}}
\end{aligned}$$

The time rate of consolidation at 50 % can now be determined, as follows in Equation (5.10).

$$\begin{aligned}
\frac{T_{50,3D}}{T_{50,1D}} &= \frac{c_{v,1D}}{c_{v,3D \text{ equiv}}} & (5.10) \\
\frac{T_{50,3D}}{0.049} &= \frac{8.120 \frac{\text{m}^2}{\text{yr}}}{44.530 \frac{\text{m}^2}{\text{yr}}}
\end{aligned}$$

$$T_{50,3D} = 0.0089$$

The resulting time factor of 0.0089 is in close agreement with the expected value of 0.009, as detailed through theoretical investigation, evident in Section 3.2. The true coefficient of consolidation for this loading increment can now be determined using this time factor. This is evident in the process of Equation (5.11), and using the relationship described in Equation (5.4).

$$\begin{aligned}
c_v &= \frac{T_{50,3D} H^2}{t_{50,3D}} & (5.11) \\
&= \frac{0.0089 (58.805)^2}{2.00} \times 24 \times 60 \times 365 \times \frac{1}{1000^2} \\
&= 8.088 \frac{\text{m}^2}{\text{yr}}
\end{aligned}$$

From this, it can be seen that the vertical coefficient of consolidation of three dimensional consolidation is very close to the one dimensional coefficient of consolidation, as expected. The difference can be attributed to the subjectivity when using a graphical method. As the Casagrande factor increases to 4.38, without exact measuring techniques, inconsistencies are easy to obtain.

5.4.2 Experimental Results of the Time Factor of Three Dimensional Consolidation ($T_{50,3D}$)

The time factor of three dimensional consolidation was determined using all combinations of a three dimensional data set, and various one dimensional coefficient of consolidation values, using Equation (3.6). This was completed for both Casagrande's and Taylor's method. The resulting time factors were graphed against the pressure at which they corresponded to, in order to determine if a relationship was evident.

The time factors determined using Casagrande's and Taylor's Methods are evident in Figure 5.3 and Figure 5.4 respectively. From these graphs, it is evident that as the load applied to the sample increases, the three dimensional time factor increases, resulting in a reduction in the coefficient of horizontal consolidation. This indicates a more anisotropic sample in the early stages of consolidation. A representative set of data for the time factor is evident in Appendix D-2.

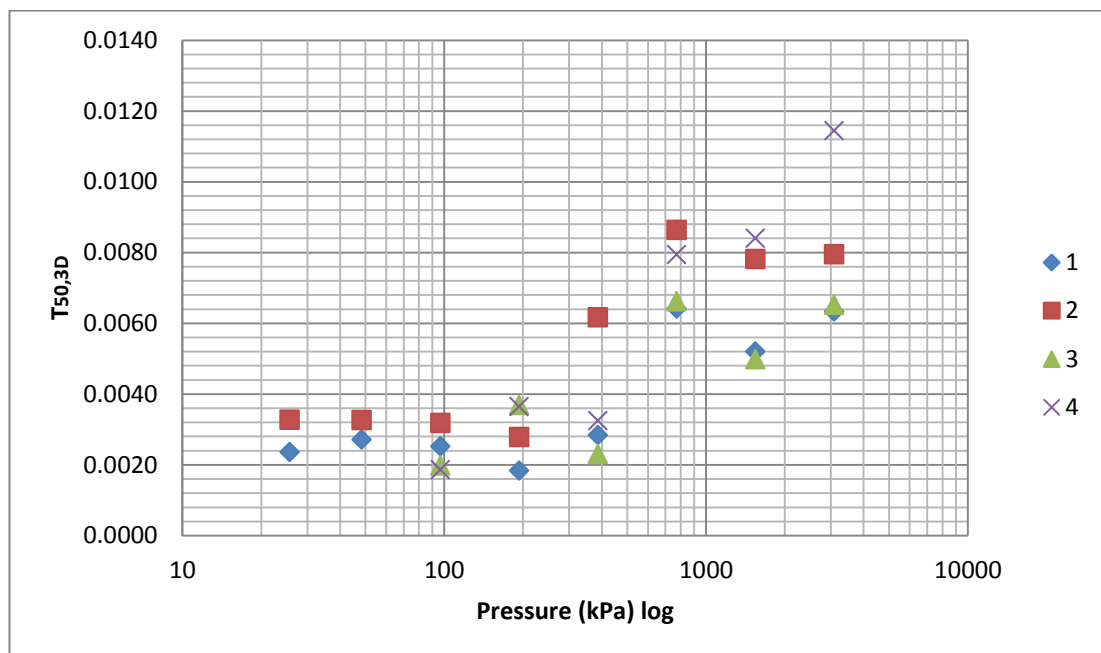


Figure 5.3: Three Dimensional Casagrande's Method Time Factors Using Experimental Data

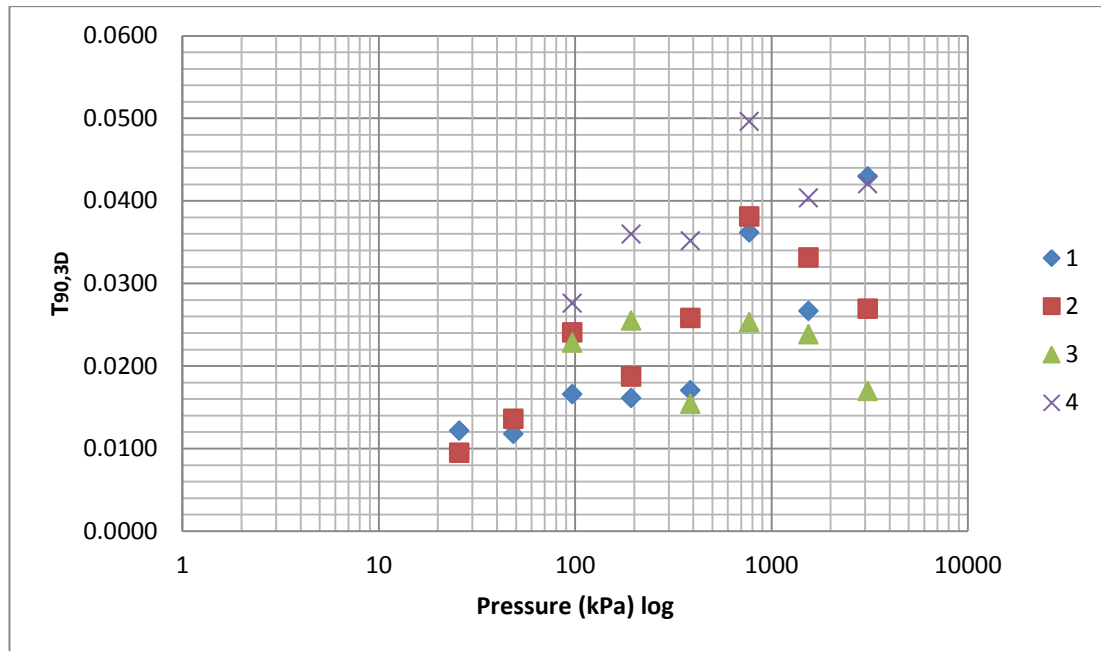


Figure 5.4: Three Dimensional Taylor's Method Time Factors Using Experimental Data

5.5 Determining the Horizontal Coefficient of Consolidation

To quantify the horizontal coefficient of consolidation, the graphs presented in Section 3.2 are used. The relationship between the time factor of three dimensional consolidation, the radius and height of the sample, and the coefficient of vertical and horizontal consolidation allows the anisotropy of a sample to be determined. The example previously presented for Casagrande's method will be continued to provide further understanding of this methodology.

The time factor of three dimensional consolidation, of 0.0089 as determined earlier, was drawn onto Figure 5.5 until the curve was reached. The corresponding radial factor ($\frac{R}{H} \times (\frac{c_v}{c_h})^{0.5}$) value was determined.

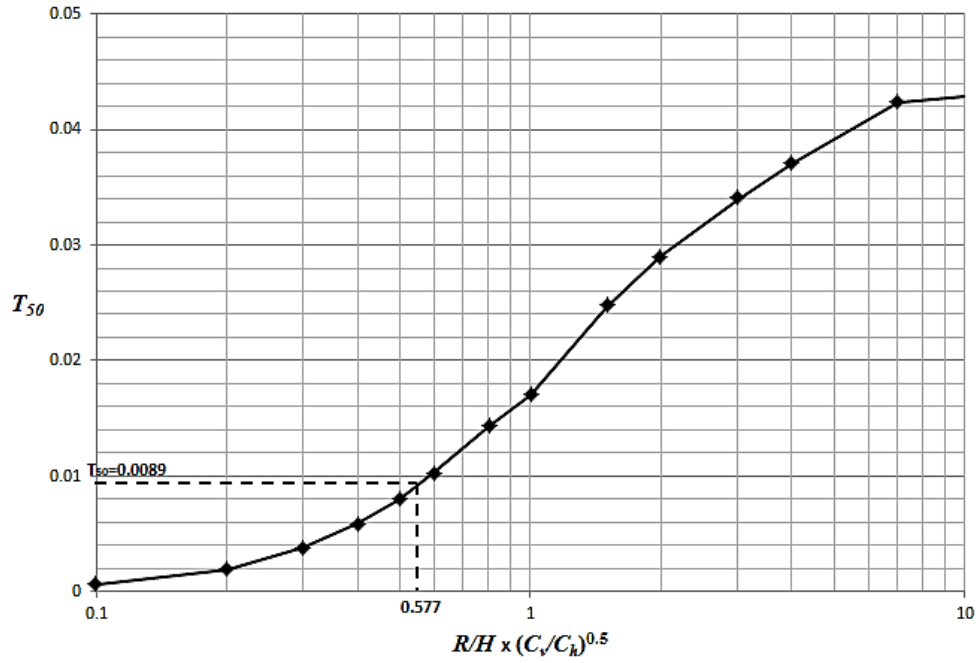


Figure 5.5: Determining the Horizontal Coefficient of Consolidation

The radial factor was determined as 0.577. This was used to express a relationship between the horizontal coefficient of consolidation, and vertical coefficient of consolidation, as represented in Equation (5.12).

$$0.577 = \frac{R}{H} \times \left(\frac{c_v}{c_h}\right)^{0.5} \quad (5.12)$$

$$0.577 = \frac{\left(\frac{63}{2}\right)}{58.805} \times \left(\frac{c_v}{c_h}\right)^{0.5}$$

$$0.577 = 0.536 \times \left(\frac{c_v}{c_h}\right)^{0.5}$$

$$c_h = 0.863c_v$$

As the vertical coefficient of consolidation for this loading increment is known to be 8.088 m²/yr, the coefficient of consolidation in the horizontal direction can be quantified, shown following in Equation (5.13).

$$c_h = 0.863c_v \quad (5.13)$$

$$c_h = 0.863 \times 8.088 \frac{m^2}{yr}$$

$$c_h = 6.980 \frac{m^2}{yr}$$

A horizontal coefficient of consolidation value that is the same as the vertical coefficient of consolidation ($c_h = c_v$) is expected for an isotropic sample. This relies on a perfectly undisturbed sample, however is often difficult to obtain in the methods used to extrude the sample.

5.5.1 Method to determine the Radial Factor with an input of time factor using MATLAB

A large quantity of data was obtained for three dimensional consolidation, and hence, a large number of calculations to determine the horizontal coefficient of consolidation. In order to ensure greater accuracy with the coefficient of consolidation results obtained, rather than reading values off the plot of Figure 3.2 and Figure 3.3 for Casagrande's and Taylor's method respectively and for ease of calculation when determining the radial factor from the time factor values, a MATLAB code was developed. Unfortunately a simple curve fit could not be achieved, resulting in the need for a polynomial curve fit.

To accurately fit a curve to the data points, a polynomial curve fit of degree eleven was required for both Taylor's and Casagrande's Methods. This provided accuracy to 1.0×10^{-4} of the R/H values between 0.1 and 0.6, and an accuracy of 1.0×10^{-3} for the R/H values ranging between 0.8 and 1.0.

This code relied on treating the R/H value as a function of the time factor. This allowed inputs of time factor values, with an output of the radial time factor. The MATLAB code for both Casagrande's and Taylor's Method is evident in Appendix B-4.

5.5.2 Comparison Between Horizontal Coefficient of Consolidation of Casagrande's and Taylor's Method

The horizontal coefficient of consolidation was determined using both Casagrande's and Taylor's method, with a sample of results evident in Figure 5.6. It is evident in this figure, that the horizontal coefficient of consolidation is larger when using Taylor's method compared to Casagrande's method. This was expected, as the relationship to determine the horizontal coefficient of consolidation depends on the vertical coefficient of consolidation, which is larger for Taylor's method than Casagrande's method.

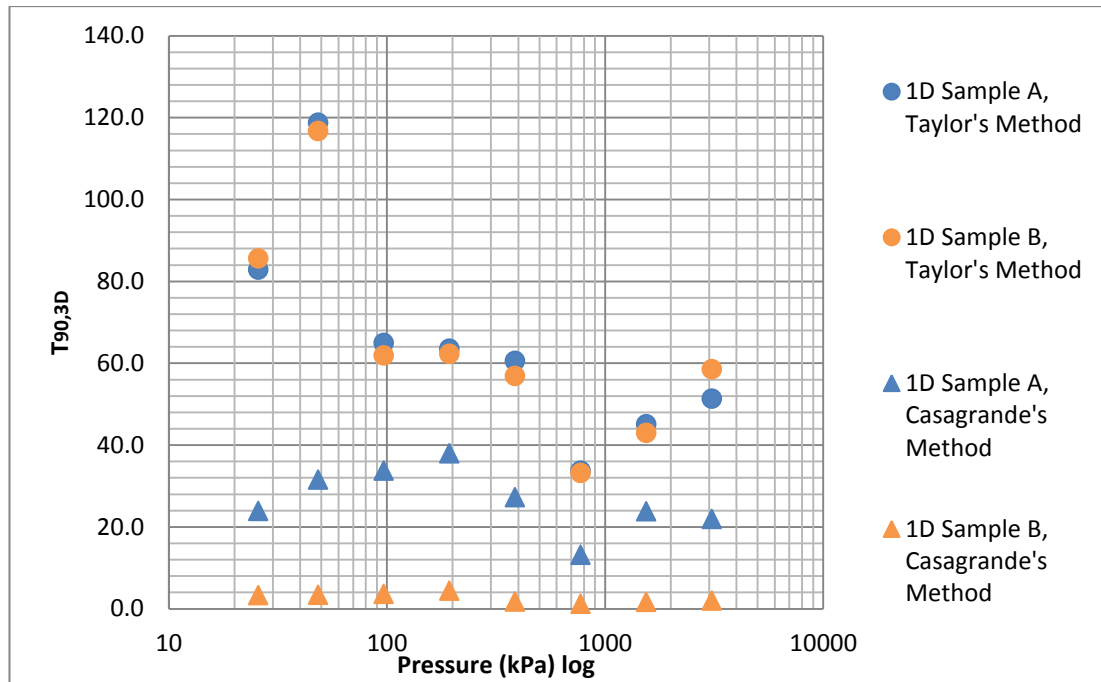


Figure 5.6: Comparison of Horizontal Coefficient of Consolidation obtained using Casagrande's and Taylor's Method

5.5.3 Comparison Between Horizontal Coefficient of Consolidation and Vertical Coefficient of Consolidation

Casagrande's Method

The horizontal coefficient of consolidation obtained using Figure 3.2 for Casagrande's method has been determined for the experimental results with a common range between one (1) and four (4) times that of the vertical coefficient of consolidation experienced. This is depicted in Figure 5.7.

When observing Figure 5.7 it appears that, to the point of the preconsolidation pressure (160 kPa in this instance), the horizontal coefficient of consolidation is increasing, as is the vertical coefficient of consolidation. After the preconsolidation pressure however, it appears that the horizontal coefficient of consolidation decreases, whereas the vertical coefficient of consolidation increases.

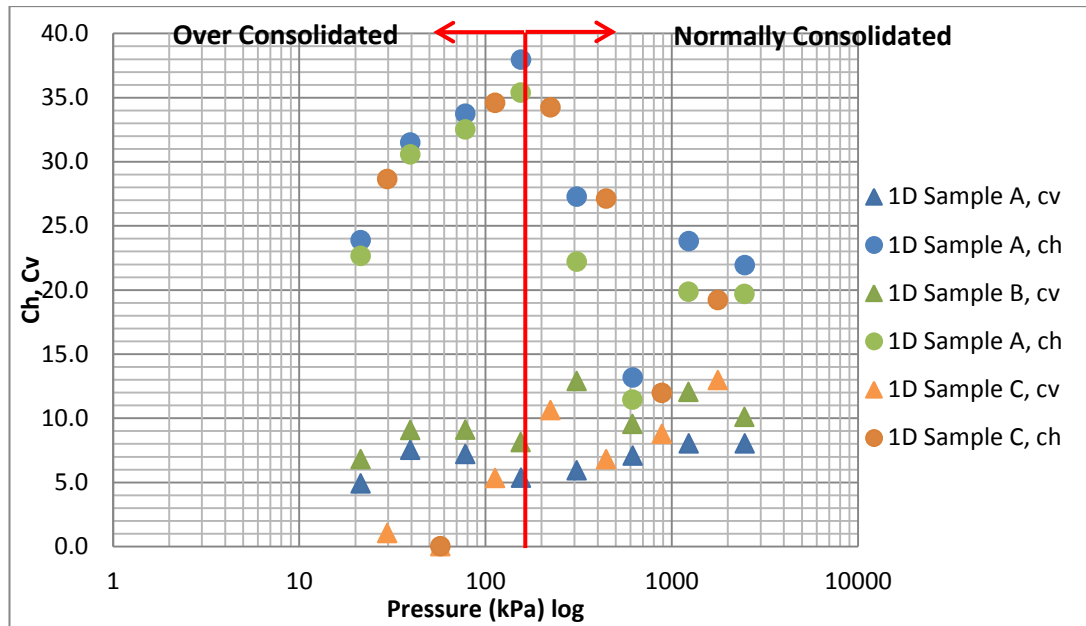


Figure 5.7: Comparison between the Horizontal Coefficient of Consolidation and Vertical Coefficient of Consolidation – Casagrande's Method

Taylor's Method

The horizontal coefficient of consolidation is compared with the vertical coefficient of consolidation in Figure 5.8 for Taylor's Method.

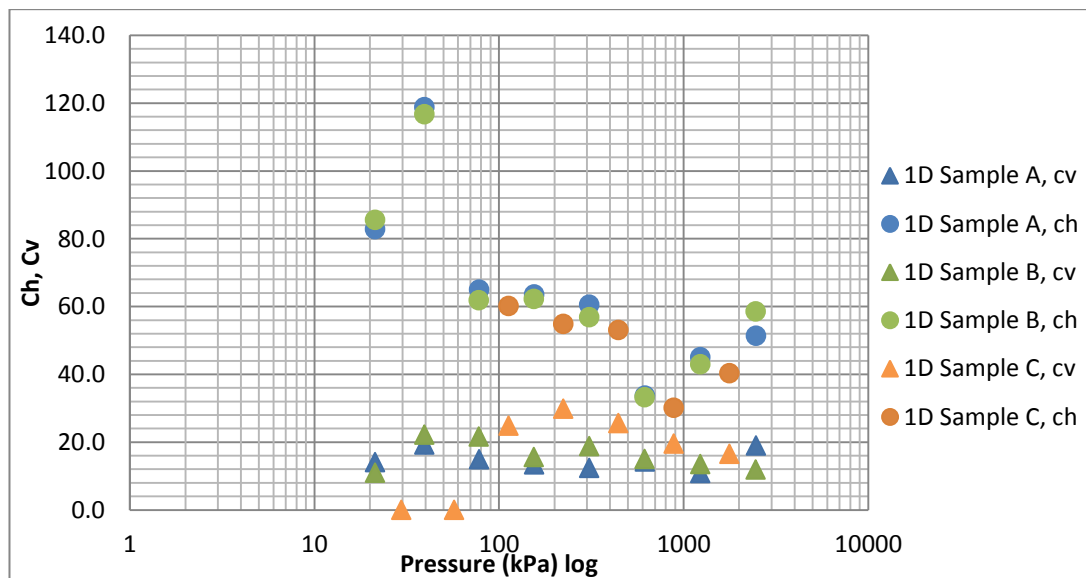


Figure 5.8: Comparison of Horizontal Coefficient of Consolidation obtained using Casagrande's and Taylor's Method

The horizontal coefficient of consolidation, determined using Figure 5.8 for Taylor's method, has a general range between two (2) and six (6) times greater than that of the vertical coefficient of consolidation. This difference is slightly greater than that obtained using Casagrande's method.

5.5.4 Comparison with Literature

The experimental results presented above show that the horizontal coefficient of consolidation is greater than the vertical coefficient of consolidation, obtained through experimental investigation.

This can be attributed to an increase in anisotropic permeability, as concluded by (Razouki and Al-Zayadi 2003). Studies conducted by Clennel et al. (1999) show a permeability anisotropy for kaolinite of 1.7. As the coefficient of consolidation is proportional to the permeability, a value of 1.7 for the ratio of c_h to c_v of this kaolinite would be expected. The kaolinite used in this study had a grain size of 2.61, a liquid limit of 69 % and a plastic limit of 38 %. It is evident that the kaolinite in this study exhibited similar properties to that used within the laboratory investigations.

The experimental results obtained for Casagrande's method for the laboratory investigations show a c_h value between one (1) and four (4) times greater than that of c_v . When comparing these results to those obtained by Clennell et al. (1999), it can be seen that the permeability anisotropy observed through experimental results corresponds, however also experiences greater anisotropy.

5.6 Comparison between Analytical and Experimental Average Degree of Consolidation (U-T) Curves

The average degree of consolidation curves determined from the analytical solution can be verified for one and three dimensional consolidation using experimental data.

Figure 5.9 shows the average degree of consolidation curve of the analytical solution of a radius/height (R/H) value of infinity, simulating a scenario of a consolidating layer of large width, compared to height. As expected, the one dimensional experimental data aligns with this curve.

The figure also presents the average degree of consolidation curve of a R/H value of 0.5 and 0.7. Initially, the three dimensional consolidation sample had a R/H value of 0.5, however, as the height of the sample decreased with increasing load, the R/H value increased to

approximately 0.7. Therefore it was expected that the three dimensional consolidation experimental data would fall between this range. As evident in Figure 5.9, the experimental data falls between this range, and hence, the analytical solution is validated.

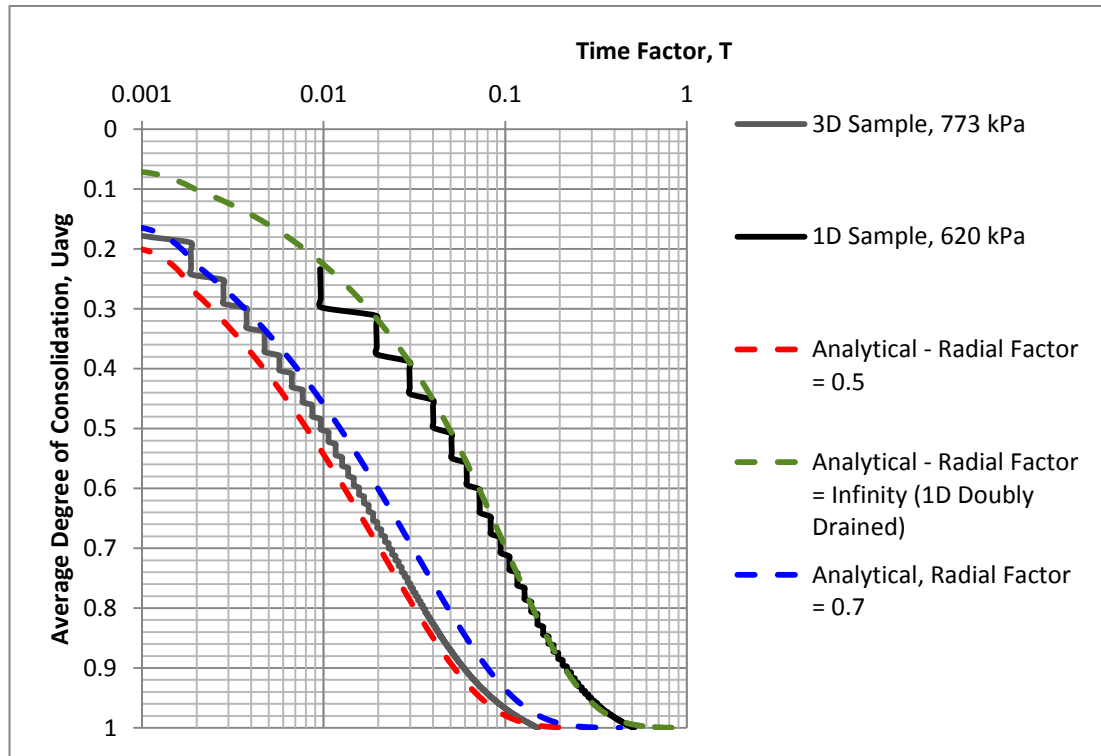


Figure 5.9: Average Degree of Consolidation (U-T) Curves for One and Three Dimensional Consolidation – Verification of Analytical Solution Using Experimental Data

5.7 Scanning Electron Microscope (SEM) Images – Analysing Particle Orientation

Scanning Electron Microscope (SEM) images were obtained through the Advanced Analytical Centre at James Cook University. From these images, observations can be made with respect to particle orientation and alignment. SEM images were obtained for a selection of samples, including after sample preparation, and after the standard oedometer. These are explained following.

5.7.1 SEM Image – After Sample Preparation

A SEM image, as shown in Figure 5.10 was obtained for a sample after preparation in the tall oedometer. A load ranging from 0 to 160 kPa was applied to the clay slurry with an

initial water content of 148 %, contained within the tall oedometer. The final water content at extrusion of the sample after preparation was 67 %.

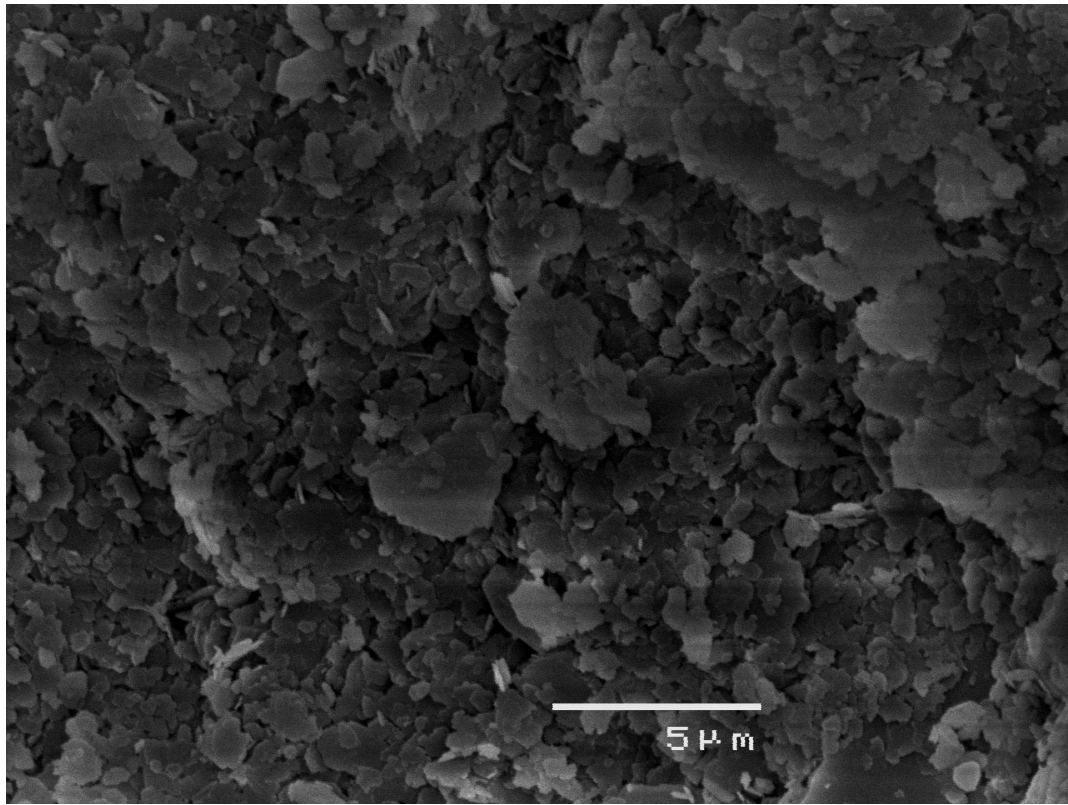


Figure 5.10: SEM Image – After Tall Oedometer (Top View)

When observing Figure 5.10, it appears that an anisotropic particle arrangement is present, as the particles show random orientation.

5.7.2 SEM Image – After Standard Oedometer

Figure 5.11 shows the particle alignment having occurred after a one dimensional consolidation test, loaded to 160 kPa, and unloaded. When observing this figure, it appears that the particles have partially aligned to the direction normal to the stress. This may be attributed to stress induced anisotropy.

Figure 5.12 shows the SEM image obtained for a one dimensional, vertically cut sample. When observing this, it appears that many of the particles are oriented parallel to the direction of load applied. This is expected due to the location of the cut sample. It would be expected, that with considerable time and stress, the particles would rotate to align normal to the load, in a more stable arrangement (Sivakugan et al. 1993).

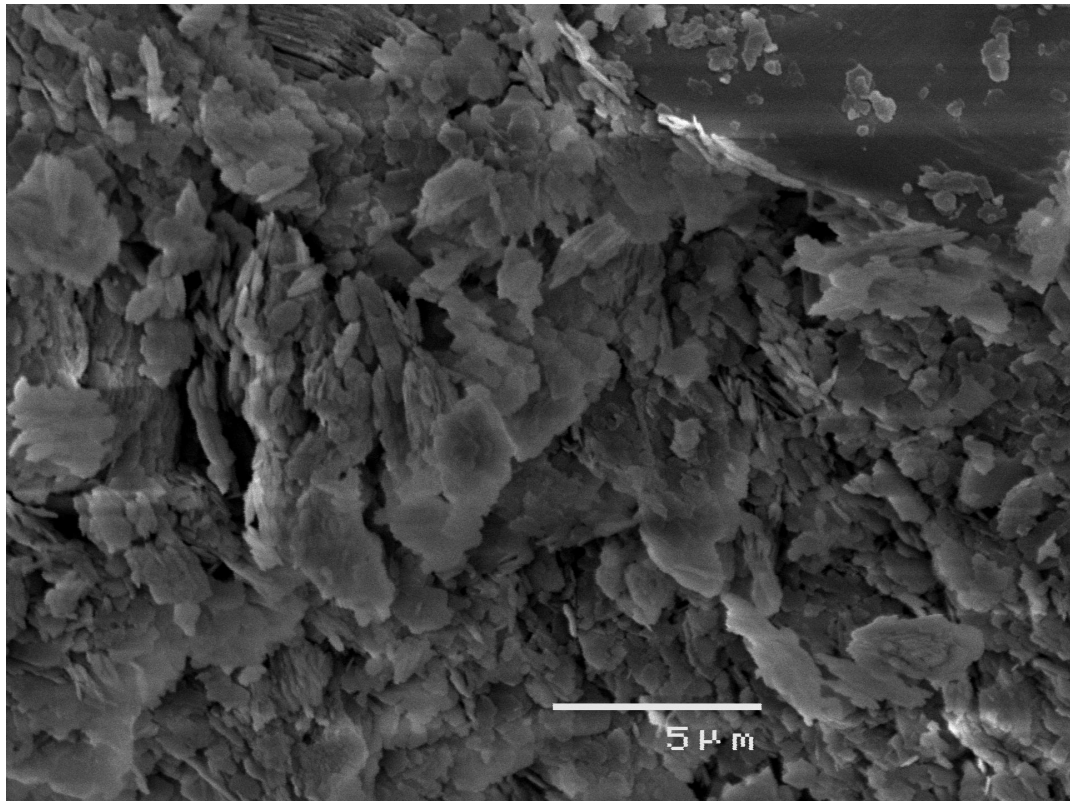


Figure 5.11: SEM Image – After Standard Oedometer for One Dimensional Horizontally Cut Sample

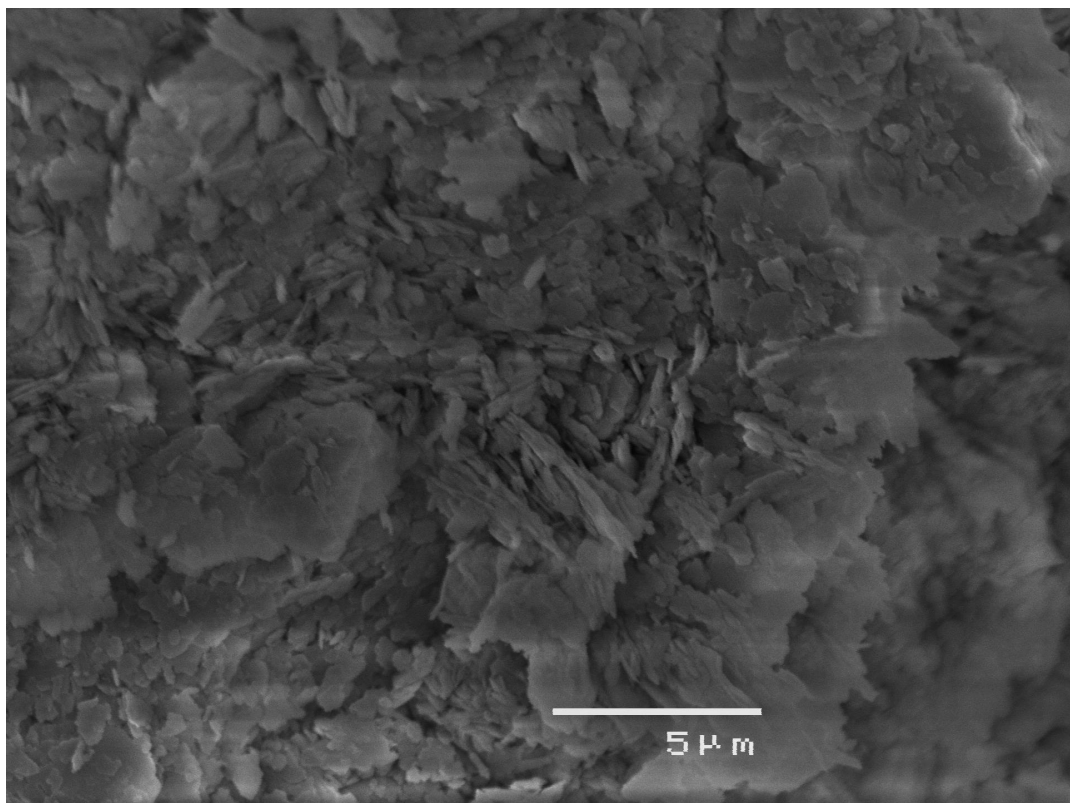


Figure 5.12: SEM Image – After Standard Oedometer on a Vertically Cut Sample.

Figure 5.13 portrays the SEM scan obtained after the standard oedometer on a three dimensional consolidation sample. This sample was loaded to 160 kPa, however not unloaded. When observing this figure, it appears that an anisotropic sample exists due to the various alignments of the particles. It does however, appear that the particles are further aligned with the direction normal to the applied load, than observed in Figure 5.10, the particle alignment after sample preparation.

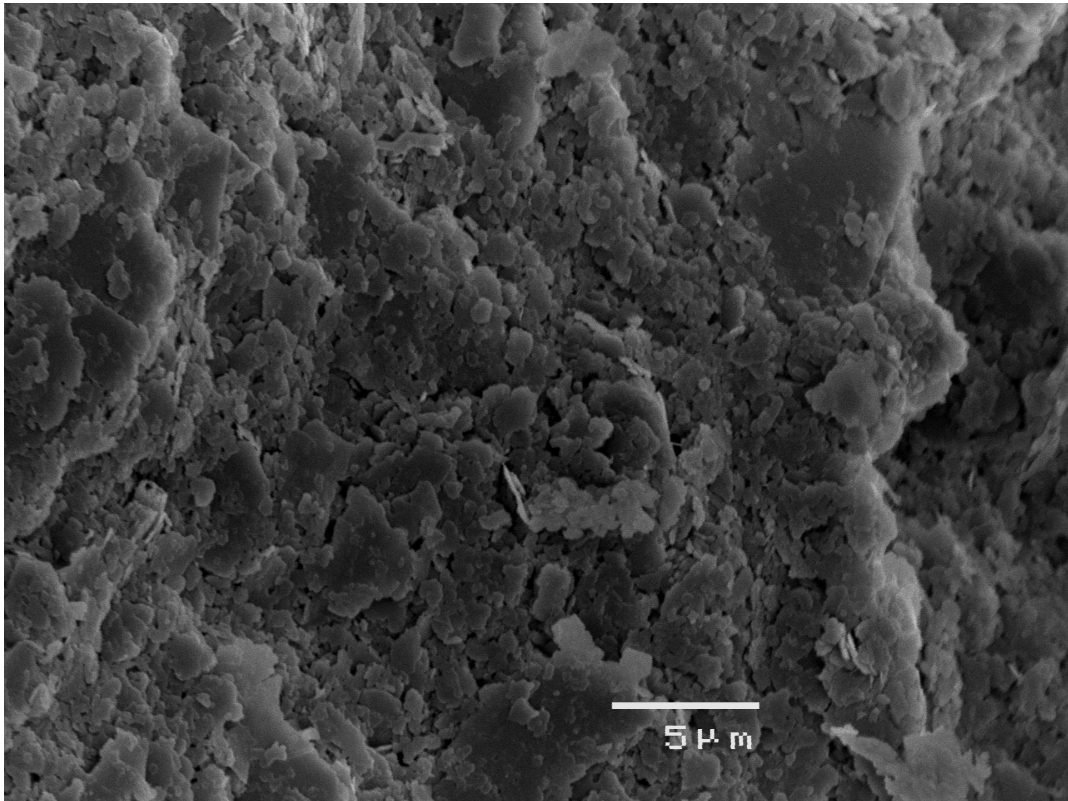


Figure 5.13: SEM Image – After Standard Oedometer of a Three Dimensional Sample

5.8 Summary

This chapter presented the results obtained for the horizontal coefficient of consolidation from extensive experimental investigation. It was evident that Taylor's method resulted in a greater coefficient of consolidation than Casagrande's method, which was to be expected as the obtained coefficient of horizontal consolidation was based upon the coefficient of vertical consolidation, which is larger for this theory. It was interesting to note that the horizontal coefficient of consolidation decreased after the preconsolidation pressure was reached, however the vertical coefficient of consolidation increased. SEM scanning was completed to observe the particle orientation in the sample to make observations with respect to anisotropy with respect to these.

Chapter 6: Further Experimental Investigation

6.1 Verification of the Coefficient of Consolidation through Falling Head Permeability Testing

The vertical and horizontal coefficient of consolidation was acquired through the use of Equation (2.13), after determining the permeability of the sample at the end of each loading increment. The samples were cut at two different configurations, one vertically and the other horizontally, depicted in Figure 4.2.

The coefficient of consolidation determined using direct permeability is compared to those obtained from the graphical methods of Taylor's and Casagrande's method, as evident in Figure 6.1.

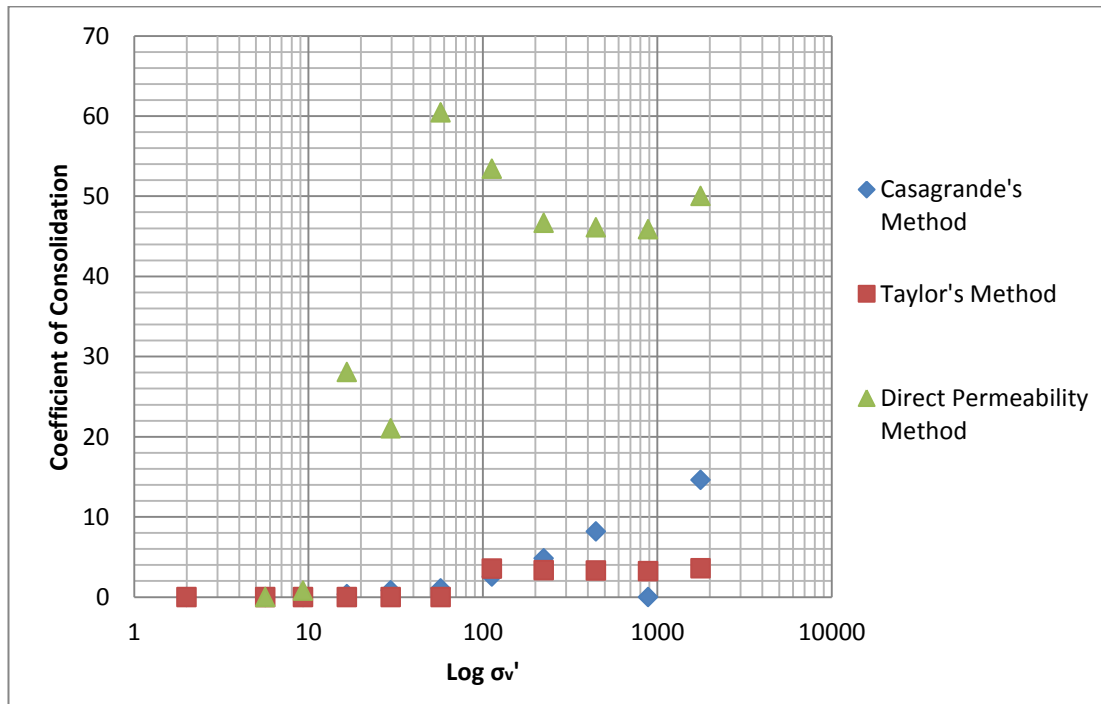


Figure 6.1: Comparison Between the Coefficient of Consolidation obtained from Taylor's and Casagrande's Method, and the Direct Determination of Permeability.

Although the coefficient of consolidation, when using the direct permeability is greater than that obtained when using Taylor's or Casagrande's method, it is generally expected that this will occur, as discussed in Al-Tabbaa and Wood (1987).

Al-Tabbaa and Wood (1987) attribute this to the effective stress variation across the sample, particularly at the drainage boundaries, which results in an increase in void ratio in these regions, and hence excess dissipation. It is noted by Pane et al. (1983), that falling head

permeability tests attain greater accuracy over an increased time period, achieving a result in close proximity to the more accurate permeability determination method of a flow pump. Flow pumps are able to measure very low flow rates (Al-Tabbaa and Wood 1987).

6.2 Creep Estimation

Creep was analysed with respect to all settlement-time plots obtained, with results evident in Figure 6.2. When observing this figure, it appears that initially, before the preconsolidation pressure is reached, the one and three dimensional consolidation tests have similar values of creep. After the preconsolidation pressure, both the one and three dimensional creep values increase, with the three dimensional creep value increasing by a large amount compared to the one dimensional creep values.

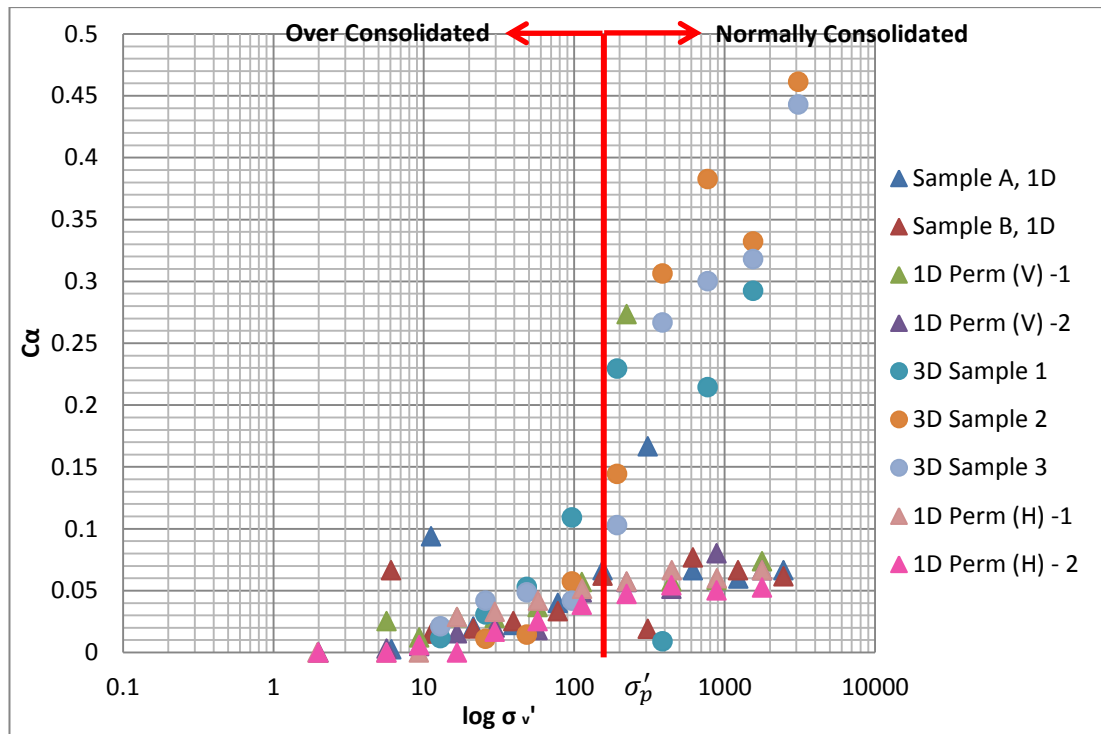


Figure 6.2: Comparison of Coefficient of Secondary Consolidation (c_α) for Three Dimensional and One Dimensional Consolidation

6.2.1 Comparison with Literature

It was expected that the value of creep would increase after the preconsolidation pressure was reached. This is documented by Craig (1978), where it is noted that the creep experienced on normally consolidated clays is greater than if it was overconsolidated.

6.3 Void- $\log \sigma'_v$ Curve

Compression-Recompression curves were developed for the full range of experimental data. The results obtained followed the trend expected, such that a slope equal to the recompression index was evident until the preconsolidation pressure of 160 kPa was reached, where a steeper slope of the compression index was then experienced. These curves can be seen in Figure 6.3 and Figure 6.4 for one dimensional and three dimensional consolidation respectively.

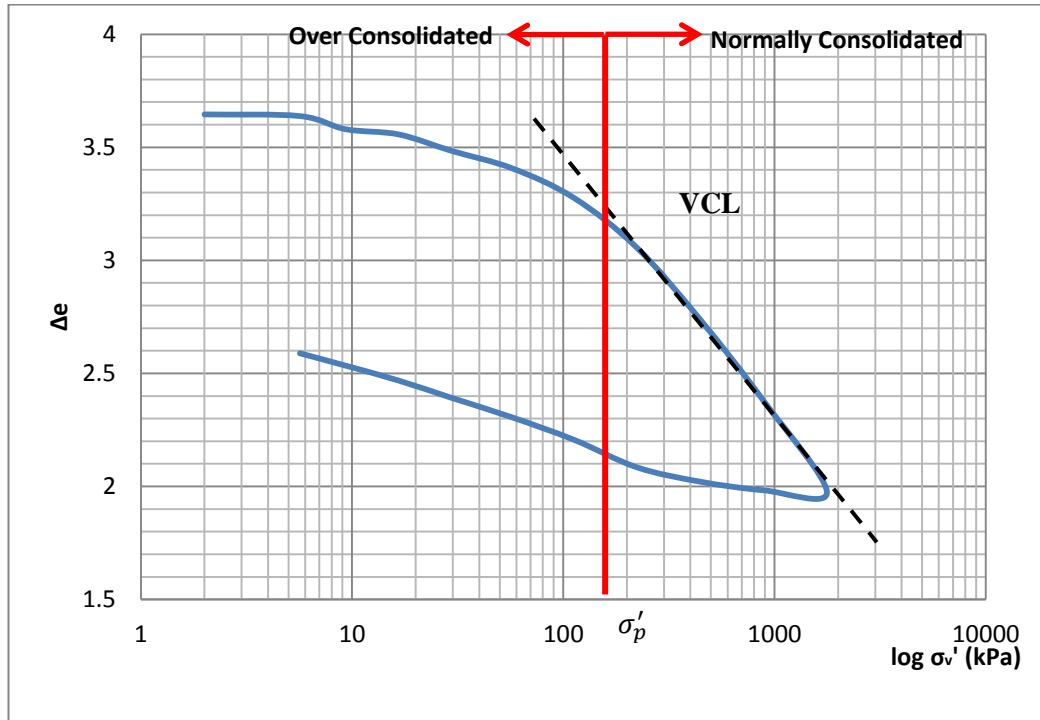


Figure 6.3: Void- $\log \sigma'_v$ Curve for One Dimensional Consolidation

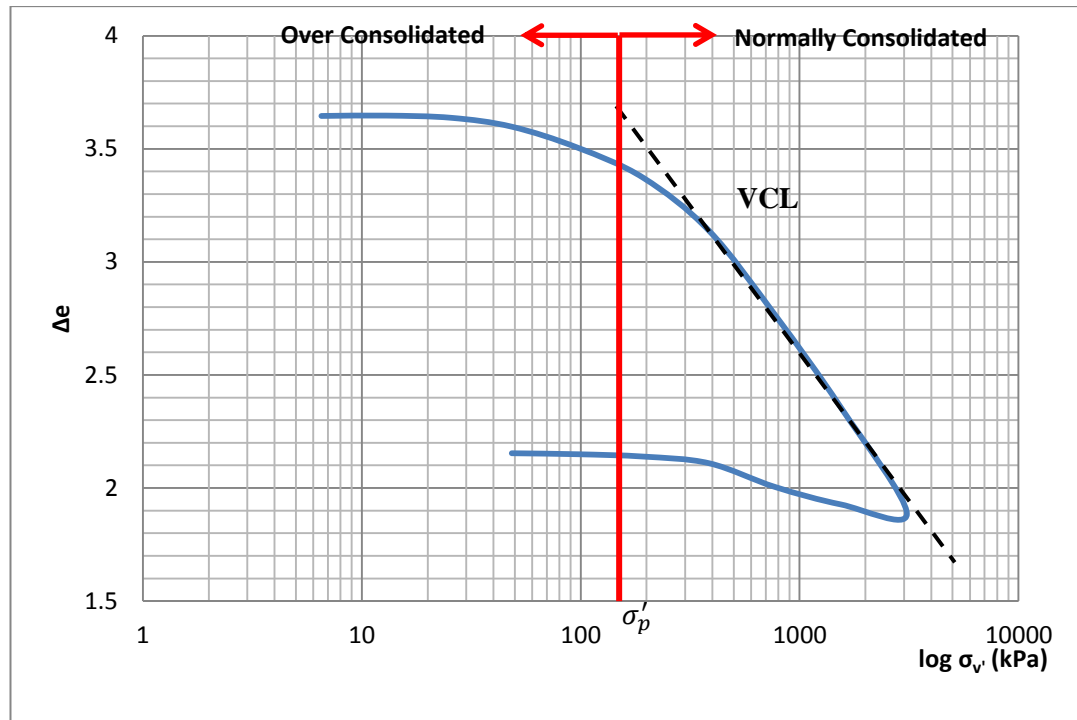


Figure 6.4: Void- $\log \sigma_v'$ Curve for Three Dimensional Consolidation

The compression and recompression index values for all tests undertaken are evident in Table 6.1. From this table, it is evident that the rate of compression for one and three dimensional consolidation are within the same range of values, however, the recompression index is lower for three dimensional samples than for one dimensional samples.

Table 6.1: Compression Index and Recompression Index Values for Experimental Results

	Compression Index (Cc)	Recompression Index (Cr)
1D, Vertically Cut Samples	1.251	0.450
	1.562	0.296
	1.508	0.386
	1.223	0.321
1D, Horizontally Cut Samples	0.587	0.319
	0.629	0.249
3D Samples	1.046	0.147
	1.329	0.287
	1.262	0.419

6.4 Summary

This chapter analysed further data obtained from experimental results, in order to achieve the sub-objectives of the project. Falling head permeability tests were conducted to make a

comparison between the coefficient of consolidation obtained using the direct permeability, and that of the graphical methods of Taylor and Casagrande. Creep was also analysed with respect to one and three dimensional consolidation, with results such that an increase in the creep values were evident after the preconsolidation pressure was reached. Furthermore, the compression-recompression curve was analysed, with comparison between one and three dimensional consolidation tests indicating a similar compression index, however a smaller recompression index resulted for three dimensional samples.

Chapter 7: Summary, Conclusions and Recommendations

The primary objective of this thesis was to quantify the rate of three dimensional consolidation. This was achieved through both analytical and experimental components.

7.1 Calculation of the Horizontal Coefficient of Consolidation

An analytical solution for three dimensional consolidation was derived by extending Terzaghi's (1925) one dimensional consolidation theory. The analytical solution allowed an average degree of consolidation (U - T) curve to be derived for various radius/height values. Modified curve fitting parameters were proposed for these various R/H ratios.

Through a series of analysis processes, a plot was developed that quantified the anisotropy of a sample with respect to the time factor at either 50 % consolidation or 90 % consolidation for Casagrande's and Taylor's method respectively.

Both the modified curve fitting parameters and standard parameters were used to determine the horizontal coefficient of consolidation, of Taylor's and Casagrande's method. When using the modified method for three dimensional consolidation, it was evident that the domain was significantly decreased to the standard curve fitting method, such that a reduction from approximately 60 % to 30 % resulted.

It was shown that when using Casagrande's method, a large difference in the horizontal coefficient of consolidation resulted between the modified and standard curve fitting process. Therefore, in order to accurately calculate the time factor and height at 50 % consolidation for three dimensional consolidation, the modified curve fitting values must be used.

When using Taylor's method to calculate the horizontal coefficient of consolidation, the portion of the straight line curve region was significantly reduced. While greater subjectivity of the straight line portion of the curve resulted, very little difference of the coefficient of consolidation resulted between the modified method and the unmodified method.

It was observed however, the coefficient of consolidation of many of the early load increments could not be quantified, due to the inability to connect the straight line portion to the initial point on the curve.

Therefore, it is recommended that the standard curve fitting parameters of Taylor's method is used to determine the coefficient of consolidation of three dimensional consolidation, however, it is possible that early increments will be unable to be used.

7.2 Creep Estimation

Through the analysis of creep from the settlement-time graphs of one dimensional and three dimensional consolidation, it was evident that initially, the creep was similar for one and three dimensional consolidation, however as the preconsolidation pressure was reached, the creep values increased. The creep of the three dimensional consolidation after preconsolidation pressure however was much greater than that of one dimensional consolidation.

This indicates that it is possible that the drainage conditions on the sample have an effect on the creep of the clay. It is recommended that further work is completed into this in order for total settlement of a three dimensional clay layer to be quantified.

7.3 Compression-Recompression Curves

The compression and recompression index for both one dimensional and three dimensional consolidation were analysed in this thesis. It was evident that the compression index of both one dimensional and three dimensional consolidation was similar, however the recompression index differed substantially.

It is recommended that further work is completed on this to determine a relationship between the one and three dimensional compression and recompression index.

References

- AS1726-1993: Geotechnical Site Investigations
- AS1289.6.6.1-1998: Soil strength and consolidation tests-Determination of the one dimensional consolidation properties of a soil-Standard Method
- Abousleiman, Y., Cheng, A.-D., Cui, L., Detournay, E. & Roegiers, J.-C. (1996). "Mandel's problem revisited." *Geotechnique* 46(2): 187-195.
- Al-Tabbaa, A. & Wood, D. M. (1987). "Some measurements of the permeability of kaolin." *Geotechnique* 37(4): 499-514.
- Asaoka, A. (1978). "Observational procedure of settlement prediction." *Soils and foundations* 18(4): 87-101.
- Aysen, A. (2002). *SOIL MECHANICS Basic Concepts and Engineering Applications*. The Netherlands, A.A Balkema Publishers.
- Barnes, G. E. (1995). *Soil Mechanics, Principles and Practice*. Palgrave.
- Barron, R. (1948). "The influence of drain wells on the consolidation of fine-grained soils." Diss., Providence, US Eng. Office.
- Bartholomeeusen, G., Sills, G., Znidarcic, D., Van Kesteren, W., Merckelbach, L., Pyke, R., Carrier, W., Lin, H., Penumadu, D. & Winterwerp, H. (2002). "Sidere: numerical prediction of large-strain consolidation." *Geotechnique* 52(9): 639-648.
- Biot, M. A. (1941). "General Theory of Three Dimensional Consolidation." *Journal of Applied Physics* 12(2): 155-164.
- Borges, J. L. (2004). "Three-dimensional analysis of embankments on soft soils incorporating vertical drains by finite element method." *Computers and Geotechnics* 31(8): 665-676.
- Carrillo, N. (1942). "Simple two and three dimensional cases in the theory of consolidation of soils." *Journal of Mathematics and Physics* 21(1): 1-5.
- Casagrande, A. & Fadum, R. (1940). "Notes on Soil Testing for Engineering Purposes " Harvard University Graduate School of Engineering Publication 268.
- Casagrande, A. & Fadum, R. E. (1900). "Notes on soil testing for engineering purposes."
- Clennell, M., Dewhurst, D., Brown, K. & Westbrook, G. (1999). "Permeability anisotropy of consolidated clays MB CLENELL1, DN DEWHURST2, KM BROWN3 & GK WESTBROOK4." *Muds and Mudstones: Physical and fluid-flow properties* 158: 79.
- Coduto, D. P. (1998). *Geotechnical Engineering: Principles and Practices*. United States of America, Prentice Hall.
- Craig, R. F. (1978). *Soil mechanics*.
- Das, B. M. (1984). *Principles of Geotechnical Engineering*. Thompson Canada Limited, Chris Carson.
- Davis, E. H. & Poulos, H. G. (1972). "Rate of settlement under two- and three-dimensional conditions." *Geotechnique* 1(22): 95-114.
- Duncan, J. M. (1993). "Limitations of conventional analysis of consolidation settlement." *Journal of Geotechnical Engineering* 119(9): 1333-1359.
- Ganesalingam, D., Ameratunga, J., Schweitzer, G., Boyle, P. & Sivakugan, S. Anisotropy in the permeability and consolidation characteristics of dredged mud. ANZ 2012 Conference Proceedings. *Ground Engineering in a Changing World: 11th Australia -*

- New Zealand Conference on Geomechanics 2012a Melbourne, VIC, Australia pp. 752-757.
- Ganesalingam, D., Sivakugan, N. & Ameratunga, J. 2012b. *Influence of settling behavior of soil particles on the consolidation properties of dredged clay sediment.*
- Gibson, R. E., Schiffman, R. L. & Cargill, K. W. (1981). "The theory of one-dimensional consolidation of saturated clays. II. Finite nonlinear consolidation of thick homogeneous layers." *Canadian Geotechnical Journal* 18(2): 280-293.
- Graham, J. & Houlsby, G. T. (1983). "Anisotropic elasticity of a natural clay." *Geotechnique* 33(2): 165-180.
- Hong, H. & Shang, J. (1998). "Probabilistic analysis of consolidation with prefabricated vertical drains for soil improvement." *Canadian geotechnical journal* 35(4): 666-667.
- Hwang, C., Morgenstern, N. & Murray, D. (1971). "On solutions of plane strain consolidation problems by finite element methods." *Canadian Geotechnical Journal* 8(1): 109-118.
- Janbu, N. (1965). "Consolidation of clay layers based on non-linear stress-strain."
- Leonards, G. (1976). "Estimating consolidation settlements of shallow foundations on overconsolidated clay." *Transportation Research Board Special Report* (163).
- Lovisa, J., Read, W. & Sivakugan, N. (2010). "Consolidation behavior of soils subjected to asymmetric initial excess pore pressure distributions." *International Journal of Geomechanics* 10(5): 181-189.
- Lovisa, J., Read, W. & Sivakugan, N. (2012). "Calculating c_v based on non-uniform initial excess pore pressure." *Geotechnique* 62(8): 741-748.
- Lovisa, J. 2013. *An Insight into Time Rate of Consolidation, PHD Thesis.* James Cook University.
- Lovisa, J., Read, W. & Sivakugan, N. (2013). "Time Factor in Consolidation: Critical Review." *International Journal of Geomechanics* 13(1): 83-86.
- Lovisa, J. & Sivakugan, N. "Tall Oedometer Testing: A Method to account for wall friction."
- Lovisa, J. & Sivakugan, S. (2013). "An in-depth comparison of c_v values determined using common curve-fitting techniques." *Geotechnical Testing Journal* 36: 1-10.
- Lovisa, J., Thomas, S., Macdonald, S. & Sivakugan, N. (2014). "A Method to Determine c_h using Three Dimensional Consolidation " *ASTM Geotechnical Testing Journal*.
- Mei, G.-X. & Chen, Q.-M. (2013). *Solution of Terzaghi one-dimensional consolidation equation with general boundary conditions.* Central South University Press and Springer-Verlag Berlin Heidelberg
- Mesri, G., Feng, T. & Shahien, M. (1999). "Coefficient of consolidation by inflection point method." *Journal of geotechnical and geoenvironmental engineering* 125(8): 716-718.
- Murray, R. (1978). "Developments in Two and Three-Dimensional Consolidation Theory." *Developments in Soil Mechanics*–1.
- Pane, V., Croce, P., Znidarcic, D., Ko, H., Olsen, H. & Schiffman, R. L. (1983). "Effects of consolidation on permeability measurements for soft clay." *Geotechnique* 23(1).
- Peng, D. X. (2011). GLINSKI, J., HORABIK, J. & LIPIEK, J. The Netherlands, Springer. 55-57.
- Poulos, H. G. & Davis, E. H. (1968). "The Use of Elastic Theory for Settlement Prediction Under Three-Dimensional Conditions." *Géotechnique* 18(1): 67-91.

- Razouki, S. S. & Al-Zayadi, A. A. (2003). "Design Charts for 2D Consolidation under Time-Dependent Embankment loading." *Quarterly journal of engineering geology and hydrogeology* 36(3): 245-260.
- Rendulic, L. 1937. *Ein Grundgesetz der Tonmechanik und sein experimenteller Beweis*. Springer.
- Sivakugan, N., Chameau, J. & Holtz, R. (1993). "Anisotropy studies on cuboidal shear device." *Journal of geotechnical engineering* 119(6): 973-983.
- Sivakugan, N. & Das, B. M. (2009). *Geotechnical engineering: a practical problem solving approach*. J Ross Pub.
- Sridharan, A., Murthy, N. & Prakash, K. (1987). "Rectangular hyperbola method of consolidation analysis." *Geotechnique* 37(3): 355-368.
- Taylor, D. W. (1948). "Fundamentals of soil mechanics." *Soil Science* 66(2): 161.
- Terzaghi, K. (1925). *Erdbaumechanik auf bodenphysikalischer Grundlage*. F. Deuticke Vienna.
- Terzaghi, K. & Frolich, O. (1936). "Theory of settlement of clay layers." Leipzig: Franz Deuticke.
- Ti, K. S., Huat, B. B., Noorzaei, J., Jaafar, M. S. & Sew, G. S. (2009). "A review of basic soil constitutive models for geotechnical application." *Electronic Journal of Geotechnical Engineering* 14: 1-18.
- Todokoro, H. & Ezumi, M. (1999). *Scanning electron microscope*. Google Patents.
- Winterkorn, H. F. & Fang, H.-Y. (1990). *Foundation Engineering Handbook*. United States of America, Kluwer Academic Publishers.

Appendix A: Derivation of Terzaghi's Equation for Doubly Drained Clay Layers

The partial differential equation to quantify the rate of one dimensional consolidation, as proposed by Terzaghi, with the assumptions listed in Section 2.5 is evident in Equation (7.1).

$$\frac{\partial u}{\partial t} = c_v \frac{\partial^2 u}{\partial z^2} \quad (7.1)$$

In this derivation, two-way drainage will be considered incorporating the modified time factor (T^*) as proposed by (Lovisa et al. 2010). This time factor is not dependent upon the length of the drainage path as discussed in Section 2.5. The derivation of the analytical solution of the partial differential equation is shown following.

A product form of the solution is assumed, evident in Equation (7.2).

$$u(z, t) = Z(z) \cdot T(t) \quad (7.2)$$

The first derivative with respect to time (t) and second derivative with respect to depth (z) is taken of the product form of the solution) with Equation (7.3) and Equation (7.4) resulting for these derivatives respectively.

$$\frac{\partial u}{\partial t} = Z(z) \cdot T'(t) \quad (7.3)$$

$$\frac{\partial^2 u}{\partial z^2} = Z''(z) \cdot T(t) \quad (7.4)$$

The derivatives are substituted into Equation (7.1), resulting in Equation (7.5), which is equated to a constant value (k) as each side of the equation depends on one parameter (z or t) only.

$$\frac{T'(t)}{c_v \cdot T(t)} = \frac{Z''(z)}{Z(z)} = k \quad (7.5)$$

Equation (7.5) can be separated and rearranged to obtain two ordinary differential equations (ODE), evident in Equations (7.6) and (7.7) .

$$T'(t) - c_v k T(t) = 0 \quad (7.6)$$

$$Z''(z) - kZ(z) = 0 \quad (7.7)$$

The boundary and initial conditions can then be applied to the ordinary differential equations.

Table 7.1: Boundary and Initial Conditions of One and Two-Way Drainage

	Boundary/Initial Condition	Separated Boundary/Initial Condition
<u>Initial Condition – One and Two-Way Drainage:</u> The applied pressure, at time zero, is initially carried by the pore water. Therefore, the initial pore water pressure, will be equal to the applied pressure	$u(z, 0) = \Delta\sigma_v$	$Z(z)T(0) = \Delta\sigma_v$
<u>One and Two-Way Drainage:</u> A permeable boundary exists at the top of the soil strata	$u(0, t) = 0$	$Z(0)T(t) = 0 \rightarrow Z(0) = 0$
<u>One-Way Drainage:</u> An impermeable boundary exists at the base of the soil strata.	$\frac{\partial u(H, t)}{\partial z} = 0$	$Z'(H)T(t) = 0 \rightarrow Z'(H) = 0$
<u>Two-Way Drainage:</u> A permeable boundary exists at the base of the soil strata	$u(H, t) = 0$	$Z(H)T(t) = 0 \rightarrow Z(H) = 0$

To obtain a solution, the constant (k) is required to be considered for a value greater than zero, equal to zero and less than zero. When k is greater than or equal to zero, no non-zero solutions of the ordinary differential equations result. Therefore the solution is obtained using a k value less than zero. This solution process is evident in Table 7.2.

Table 7.2: Solution Process for Terzaghi's Differential Equation

When $k < 0$:	let $k = -m^2$
Solution:	$Z(z) = A \cos mz + B \sin mz$
where A and B are constants	
<u>Two-way Drainage:</u>	
	$Z(0) = 0 \rightarrow A = 0$
	$Z(H) = 0 \rightarrow 0 = B \sin mH$
As $B \neq 0$:	$\sin mH = 0$
	$mH = 0$
	$m = \frac{n\pi}{H}$
Substituting m into k:	$k = -\frac{n^2\pi^2}{H^2}$
Therefore:	$Z_n = B_n \sin \frac{n\pi}{H} z$
Use k to find the corresponding T_n value, by substitution into Equation (7.6):	$T'_n + \frac{n^2\pi^2}{H^2} c_v T_n = 0$
Therefore:	$T_n = A_n e^{-\frac{n^2\pi^2}{H^2} c_v t}$
The time factor can be introduced using Equation	$T^* = \frac{c_v t}{H^2}$
The constants A_n and B_n can be combined into a single constant C_n .	$u_n(z, t) = C_n \sin \frac{n\pi z}{H} e^{-n^2\pi^2 T^*}$

To satisfy the initial condition, a sum of the solutions is taken:

$$u(z, t) = \sum_{n=1}^{\infty} u_n(z, t)$$

Applying the initial condition:

$$u(z, t) = C_n \sin \frac{n\pi z}{H} e^{-n^2 \pi^2 T}$$

$$u(z, 0) = \Delta\sigma_v = \sum_{n=1}^{\infty} C_n \sin \frac{n\pi z}{H}$$

This is recognized as a Fourier sine series, and hence, C_n can be expressed as:

$$C_n = \frac{1}{H} \int_0^{2H} \Delta\sigma_v \sin \frac{n\pi z}{2H} dz$$

When substituting into $u(z, t)$ equation:

$$u(z, t) = \sum_{m=1}^{\infty} \left[\frac{2\Delta\sigma_v}{m\pi} \left(1 - (-1)^m \sin\left(\frac{n\pi z}{H}\right) \right) \exp(-m^2 \pi^2 T^*) \right]$$

Appendix B: MATLAB Code

B-1: Matlab Code for Degree of Consolidation Curves

```
hold all %holding all graph properties on

%Z Factor values
Z=0:0.001:2

%Time factor values
T=0;
while T <= 2; %Graphing for a time factor less than 2

    %setting sum to 0, used as a counter
    sum=0;

    %Setting up the sum of (between m=0 to 'infinity') as the
    function converges quickly, 10 000 will obtain a suitable result
    for m=0:10000;

        %determining M factor
        M=(pi/2)*(2*m + 1);

        %letting x be the sum portion of the degree of consolidation
        equation
        x=(2/M)*sin(M*Z)*2.718281828.^(-(M^2)*T);

        %sum is a counter, adds the additional x values for each
        iteration of m
        sum=sum+x;

    end

    %determining u(z)
    uz=1-sum;

    %Plotting graph
    plot(uz,Z, 'k')

    if (T < 0.3) %setting the T increments at 0.05 when less than
0.3
        T=T+0.05;
    else
        T=T+0.1; %setting the T increments to 0.1 when greater than
0.3
    end
end

%setting up the axis
axis([0 1 0 2])
grid on % plotting grid lines
set(gca,'YDir','reverse'); %reversing the axis direction

%set(gca,'XScale','log'); %putting x axis in log scale
title('Degree of Consolidation Chart')
xlabel('Degree of Consolidation, Uz')
ylabel('Depth Factor, Z')
```

B-2: Matlab Code for Average Degree of Consolidation-Time Factor Graph

```
%setting sum to 0, used as a counter
sum=0;

%Time factor values
T=0:0.001:2

%Setting up the sum of (between m=0 to 'infinity') as the function
converges quickly, 50 000 will obtain a suitable result

for m=0:50000;

%determining M factor
    M=(pi/2)*(2*m + 1);

%letting x be the sum portion of the avg degree of consolidation
equation
    x=(2/M^2)*2.718281828.^(-(M^2).*T);

%sum is a counter, adds the additional x values for each iteration
of m
    sum=sum+x;

end

%determining u average
uavg=1-sum

%Plotting graph
plot(T,uavg, 'k')

%setting up the axis
ylim([0 1]);
axis([0 2 0 1])
semilogx(uavg); % log scale for Time factor T
grid on % plotting grid lines
set(gca, 'YDir', 'reverse'); %reversing the axis direction
set(gca, 'XScale', 'log'); %putting x axis in log scale
title('Average Degree of Consolidation Chart')
xlabel('Time factor, T')
ylabel('Average degree of consolidation, Uavg')
```

B-3: Code to determine Radial Factor with an input of Time Factor – Casagrande's Method

```
%hold all %Plotting graphs on same graph
clear all
clc
format long %Increasing the number of Decimals

%We will swap the x and y axis, such that x is T50, and y is R/H
%in order to obtain a function R/H= ...*T50.

T50actual=[0.037 0.034 0.029 0.0247 0.017 0.0143 0.0103 0.008 0.0059
0.0038 0.0019 0.00055];

RdivHactual=[4 3 2 1.5 1 0.8 0.6 0.5 0.4 0.3 0.2 0.1];

%Finding the coefficients of a polynomial to the power of 11. 11 was
chosen
%by guess and check, in order to ensure error remained low.

coefficient=polyfit(T50actual,RdivHactual,11);

%Finding the R/H values obtained with the polynomial fit

RdivHfit=polyval(coefficient,T50actual);

%Calculating the Error
Error=RdivHfit'-RdivHactual'

%Plotting the fit to actual value graphs

plot(T50actual,RdivHactual,'k.-');
plot(T50actual,RdivHfit,'r*--');

%Finding the R/H value for an input value of T50
T50=[0.0032
0.0014
0
0.0056
0.0117
0.0183
0.0146
0.0185
0.0134];

RdivHatT50=polyval(coefficient,T50);

table=[RdivHatT50]
```

B-4: Code to Determine Radial Factor with an Input of Time Factor – Taylor's Method

```
%hold all %Plotting graphs on same graph
clear all %clearing current variables saved in Matlab
clc %clearing the screen
format long %Increasing the number of Decimals

%We will swap the x and y axis, such that x is T90, and y is R/H
%in order to obtain a function R/H= ...*T90.

T90actual=[0.185 0.176 0.158 0.1418 0.11 0.0915 0.0666 0.052 0.0376
0.0235 0.0115 0.003];

RdivHactual=[4 3 2 1.5 1 0.8 0.6 0.5 0.4 0.3 0.2 0.1];

%Finding the coefficients of a polynomial to the power of 11. 11 was
chosen
%by guess and check, in order to ensure error remained low.

coefficient=polyfit(T90actual,RdivHactual,11);

%Finding the R/H values obtained with the polynomial fit

RdivHfit=polyval(coefficient,T90actual);

%Calculating the Error
Error=RdivHfit'-RdivHactual'

%Plotting the fit to actual value graphs

%plot(T90actual,RdivHactual,'k.-');
%plot(T90actual,RdivHfit,'r*--');

%Finding the R/H value for an input value of T90
T90=[0.0241
0.0348
0
0.0538
0.0384
0.0440
];

RdivHatT90=polyval(coefficient,T90);

table=[RdivHatT90]
```

Appendix C: Tall Oedometer Procedure for Preparation of Slurry Sample

The tall oedometer apparatus is initially disassembled into three components; the base, the perspex cell and the top containing the diaphragm.

1. A filter paper cut to size is placed on the base of the tall oedometer.
2. The perspex cell is placed on top of the base in line with the bolt holes. For a simple method to insert and tighten the bolts, the perspex cell is turned upside down.
3. The bolts are tightened to an even pressure, where they are then further tightened. It should be ensured that the bolts are not tightened too much as to break the perspex.
4. All drainage valves are turned 'off'.
5. The apparatus is then turned upright, and the slurry is placed into the perspex tube with a funnel and scoop. The mixture is filled to a height approximately 3 cm from the top.
6. A knife is used to mix the sample in the column, to minimise the present voids. The column is then placed on the vibratory machine for approximately 30 seconds to further remove any voids.
7. If the slurry is viscous, the following steps can be completed straight after the vibration. If the slurry however is very liquid, it is left to sit overnight where the excess water can be removed before continuing further.
8. A porous filter paper is placed on top of the sample, along with a filler stone.
Note: This stone should be porous if double drainage is required.
9. The top cap is placed on the column, with the diaphragm inserted into the top of the column, ensuring the diaphragm is at an even level (inserted properly).
10. The top bolts are inserted and evenly tightened, where further tightening can then occur.
11. The tall oedometer apparatus is placed in the triaxial apparatus, where the pressure hose (Number 2) is inserted into the pressure outlet at the top of the sample.
12. A small pressure (approximate 5 kPa) is applied (pressure valve 'open') to fill the diaphragm with water until the centre bolt hole slightly overflows.
13. The centre bolt is wrapped in plumbers tape (leak resistant) and screwed into the top. This bolt can be done up very tightly.

14. The dial gauge is placed on top of the hydraulic lever that applies pressure to record the settlement of the sample that occurs. The dial gauge is 'zeroed' at this point.
15. A small pressure of 10 kPa is applied to the sample, and the pressure valve and drainage valve is turned on 'open', where settlement of the sample can then begin.
16. It is important to ensure that the volume change dial does not exceed 4.0, in which case the pressure lever is to be turned in the opposite direction. When the dial gauge is fully extended, the reading can be recorded and the dial gauge 'zeroed'.
17. Hydraulic pressure is increased when the dial gauge reading is minimal with time. It is standard to increase in double increments. I.e. 10, 20, 40, 80, 160 kPa.
18. When approximately 30 mm of travel has occurred, a filler is required, and the apparatus is to be disassembled. The pressure is turned off, and the tap removed. The drainage tap is also turned off. The top cap is removed, and another filler placed on top. The hydraulic lever is 'oiled' to ensure constant application of pressure, and steps 10 to 14 are repeated.
19. The sample is ready for extrusion when settlement is minimal with time, and with a substantial pressure, indicating a stiff sample.

Appendix D: Experimental Results

D-1: Coefficient of Consolidation for all samples, of both Taylor's and Casagrande's method

			Casagrande's Method				Taylor's Method				Calpha	Cc	Cr
			t50	d50	H50=H0-d50	Cv (m2/yr)	t90	d90	H90	Cv			
Sample A, 1D	Top cap only	0.99											
H0=18.98	150g	6.09	1.48	0.008	18.972	6.263483723	1.55	0.027	18.953	25.82352023	0.00257		
	300g	11.19	0.8	0.064	18.916	11.5191401	1.725	0.076	18.904	23.08391866	0.093904		
	600g	21.38	1.85	0.22	18.76	4.89942796	2.76	0.29	18.69	14.10265034	0.020959		
	2.5lb	39.52	1.17	0.485	18.495	7.529640581	1.96	0.58	18.4	19.24734328	0.022146		
	5lb	78.05	1.16	0.96	18.02	7.209464715	2.38	1.13	17.85	14.9173164	0.04	1.251099	0.449784
	10lb	155.11	1.43	1.745	17.235	5.349805275	2.38	2.07	16.91	13.3875614	0.066439		
	20lb	309.23	1.13	2.84	16.14	5.937177786	2.2	3.32	15.66	12.42087102	0.166632		
	40lb	617.48	0.8	4.145	14.835	7.084946104	1.64	4.48	14.5	14.28510293	0.066439		
	80lb	1233.96	0.6	5.31	13.67	8.021160664	1.8	5.72	13.26	10.88443175	0.05979		
	160lb	2466.92	0.5	6.49	12.49	8.035377951	0.9	6.6	12.38	18.97535884	0.066439		
Sample B, 1D	Top cap only	0.99				#DIV/0!				#DIV/0!			
H0=19.82	150g	6.08				#DIV/0!	2.26	0.063	19.757	19.24530411	0.066439		
	300g	11.17	1.6	0.156	19.664	6.22408027	2.85	0.188	19.632	15.06868826	0.015078		
	600g	21.35	1.44	0.331	19.489	6.793100749	2.53	4.02	15.8	10.99473763	0.019276		
	2.5lb	39.47	1.05	0.595	19.225	9.06556413	1.84	0.668	19.152	22.21271583	0.025129		
	5lb	77.95	1	1.02	18.8	9.102635136	1.8	1.13	18.69	21.62406385	0.033219	1.56169	0.295824
	10lb	154.91	1.05	1.625	18.195	8.120191237	2.3	1.91	17.91	15.54012662	0.062034		
	20lb	308.84	0.6	2.485	17.335	12.89875751	1.7	2.88	16.94	18.80914732	0.019125		
	40lb	616.69	0.7	3.705	16.115	9.554633134	1.77	4.36	15.46	15.04654992	0.076862		
	80lb	1232.4	0.45	5.31	14.51	12.049631	1.62	5.79	14.03	13.53915453	0.066439		
	160lb	2463.81	0.46	6.39	13.43	10.09823865	1.52	7.08	12.74	11.89834303	0.06149		
1D Perm (V) -1	Top cap only	2				#DIV/0!				#DIV/0!	0		
H0=19.99	150g	5.66	1.6	0.171	19.819	6.322588677				#DIV/0!	0.025151		
	300g	9.32	1.69	0.325	19.665	5.89321972				#DIV/0!	0.012		
	600g	16.64	30	0.59	19.4	0.323097533				#DIV/0!	0.028394		
	2.5lb	29.67	10	0.922	19.068	0.936400686				#DIV/0!	0.027916		
	5lb	57.34	1.6	1.243	18.747	5.65711507	1.9	1.28	18.71	20.52982236	0.03676	1.507765	0.385529
	10lb	112.68	0.8	1.71	18.28	10.75756137	1.73	1.862	18.128	21.16629767	0.056789		
	20lb	223.35	1.44	3.575	16.415	4.819153044	2.26	4.9	15.09	11.22693628	0.273496		
	40lb	444.7	0.62	6.72	13.27	7.314785458	1.83	7.18	12.81	9.991677024	0.057227		
	80lb	887.41	0.48	8.02	11.97	7.68773669	1.52	8.47	11.52	9.728650186	0.058654		
	160lb	1772.81	0.37	9.085	10.905	8.277535507	1.54	9.81	10.18	7.498355949	0.07352		

1D Perm (V) -2	Top cap only	2	0.77	0.019	19.971	13.34013838				#DIV/0!	0		
H0=19.99	150g	5.66				#DIV/0!				#DIV/0!	0.003		
	300g	9.32	5.33	0.3005	19.6895	1.873240777				#DIV/0!	0.005026		
	600g	16.64	9.49	0.377	19.613	1.043934573				#DIV/0!	0.0153		
	2.5lb	29.67				#DIV/0!				#DIV/0!	0.02		
	5lb	57.34	1.77	0.868	19.122	5.320406286	1.64	0.885	19.105	24.79941598	0.017952	1.222903	0.321274
	10lb	112.68	0.85	1.26	18.73	10.62938324	1.3	1.32	18.67	29.87696656	0.048549		
	20lb	223.35	1.23	1.98	18.01	6.791625821	1.4	2.05	17.94	25.61580799	0.056789		
	40lb	444.7	0.85	2.965	17.025	8.782269337	1.6	3.22	16.77	19.58562162	0.051404		
	80lb	887.41	0.494	4.22	15.77	12.96545835	1.63	4.46	15.53	16.48718551	0.08		
	160lb	1772.81	0.373	5.485	14.505	14.5270714	1.2	5.85	14.14	18.5655915	0.066439		
2D Sample 1	Top cap only	0.15				#DIV/0!				#DIV/0!			
H0=63.00	150g	6.54				#DIV/0!				#DIV/0!			
	300g	12.92	0.95	0.0485	62.9515	107.4335674	3.326	0.071	62.929	32.54154109	0.011445		
	600g	25.7	0.5623	0.2725	62.7275	180.2184754	1.63	0.37	62.63	65.77122325	0.030618		
	2.5lb	48.44	1.17	0.8325	62.1675	85.07312398	2.8	1.04	61.96	37.47343349	0.052843		
	5lb	96.73	1.11	1.76	61.24	87.01594116	2.6	2.14	60.86	38.93581308	0.109163	1.046407	0.146713
	10lb	193.32	2	3.415	59.585	45.71885322	2.8	4.05	58.95	33.92097195	0.229352		
	20lb	386.49	0.85	6.25	56.75	97.58077041	3.522	8.4	54.6	23.13420789	0.009		
	40lb	772.83	1	10.625	52.375	70.64794091	3.304	12.55	50.45	21.05430949	0.21435		
	80lb	1545.51	0.5623	14.8	48.2	106.4087716	2.87	16.8	46.2	20.32641342	0.292403		
	160lb	3090.88				#DIV/0!				#DIV/0!			
2D Sample 2	Top cap only	0.15				#DIV/0!				#DIV/0!			
H0=63.00	150g	6.54				#DIV/0!				#DIV/0!			
	300g	12.92				#DIV/0!				#DIV/0!			
	600g	25.7	1	0.108	62.892	101.8690481	1.9	0.134	62.866	56.85082294	0.010924		
	2.5lb	48.44	0.741	0.4375	62.5625	136.0383696	1.333	0.51	62.49	80.06627062	0.014307		
	5lb	96.73	0.7	1.22	61.78	140.426543	2.333	1.66	61.34	44.07897679	0.057227	1.328771	0.286873
	10lb	193.32	0.657	2.575	60.425	143.1262805	2.4	3.22	59.78	40.69670798	0.144283		
	20lb	386.49	0.85	4.825	58.175	102.542829	2.503	5.8	57.2	35.72645362	0.306179		
	40lb	772.83	1.409	8.55	54.45	54.19212882	3.9	10.45	52.55	19.35260952	0.382498		
	80lb	1545.51	0.85	13.05	49.95	75.59681457	3.146	15	48	20.01623802	0.332193		
	160lb	3090.88	0.85	17.675	45.325	62.2455253	2.417	19.25	43.75	21.64403186	0.461173		
2D Sample 3	Top cap only	0.15				#DIV/0!				#DIV/0!			
H0=63.00	150g	6.54				#DIV/0!				#DIV/0!			
	300g	12.92	2.228	0.5775	62.4225	45.04209333				#DIV/0!	0.021078		
	600g	25.7	1.48	1.01	61.99	66.87025724				#DIV/0!	0.041918		
	2.5lb	48.44	1.8	1.825	61.175	53.54598198	2.4	2.04	60.96	42.31919278	0.048549		
	5lb	96.73	1.216	2.985	60.015	76.284707	1.9375	3.25	59.75	50.36082178	0.041778	1.262333	0.419181
	10lb	193.32	1	4.1	58.9	89.34742202	2.229	4.4	58.6	42.10598813	0.102808		
	20lb	386.49	3.863	6.6	56.4	21.20727834			63	#DIV/0!	0.266681		
	40lb	772.83	2.462	10.01	52.99	29.37319761	4.146	11	52	17.82526889	0.3		
	80lb	1545.51	1	13.35	49.65	63.48775091	3	14.95	48.05	21.0341143	0.318049		
	160lb	3090.88	0.5	17.325	45.675	107.4579483	2.5167	19.35	43.65	20.6916797	0.442924		

1D Perm (H)-1--C1,M	Top cap only	1.97			19.99	#DIV/0!				#DIV/0!	#NUM!		
h0=19.99	150g	5.64			19.99	#DIV/0!			19.99	#DIV/0!	#NUM!		
	300g	9.31	1.602	0.25	19.74	6.264453956			19.99	#DIV/0!	#NUM!		
	600g	16.64				#DIV/0!			19.99	#DIV/0!	0.028614		
	2.5lb	29.7	1.442	0.479	19.511	6.799003019			19.99	#DIV/0!	0.032737		
	5lb	57.43	1.448	0.783	19.207	6.561482086	1.85	0.865	19.125	5.403682946	0.041918	0.586853	0.319435
	10lb	112.88	1.602	1.314	18.676	5.607336967	1.95	1.41	18.58	4.838553062	0.051453		
	20lb	223.79	0.7	1.885	18.105	12.06008739	1.85	2.14	17.85	4.707208255	0.057227		
	40lb	445.62	0.6	2.73	17.26	12.78738582	1.58	3.01	16.98	4.987431972	0.066439		
	80lb	889.27			19.99	#DIV/0!	1.45	3.85	16.14	4.910183909	0.06		
	160lb	1776.56	0.3	4.52	15.47	20.54522062	1.18	4.82	15.17	5.330253383	0.066439		
1D Perm (H) -2 C2,M2	Top cap only	2				#DIV/0!			19.99	#DIV/0!	#NUM!		
H0=19.99	150g	5.66				#DIV/0!			19.99	#DIV/0!	#NUM!		
	300g	9.32				#DIV/0!			19.99	#DIV/0!	0.005723		
	600g	16.64	21.92	2.778	17.212	0.348075585			19.99	#DIV/0!	#NUM!		
	2.5lb	29.67	9	3	16.99	0.826029742			19.99	#DIV/0!	0.016767		
	5lb	57.34	6.5	3.377	16.613	1.093538833			19.99	#DIV/0!	0.025129	0.628771	0.249145
	10lb	112.68	2.644	3.818	16.172	2.547519113	2.01	3.86	16.13	3.537784522	0.038553		
	20lb	223.35	1.292	4.394	15.596	4.848589046	1.95	4.53	15.46	3.349986586	0.047332		
	40lb	444.7	0.7	5.08	14.91	8.179159615	1.78	5.3	14.69	3.313464252	0.054351		
	80lb	887.41			19.99	#DIV/0!	1.6	6.265	13.725	3.217832426	0.05		
	160lb	1772.81	0.3	6.95	13.04	14.59773128	1.23	7.27	12.72	3.595239374	0.052532		

D-2: Experimental Data to determine $T_{50,3D}$ and c_h

Corrected 3D using $f_c = 4.38$ while staying in 30% region																						
3D Sample 2				1D Sample A				1D Sample B				1D V Perm 1				1D V Perm 2						
Pressure (kPa)	cv,3Dequiv	H	R/H	cv	T50 3D	$R/H^*(cv/ch)^{0.5}$	x	ch	cv	T50 3D	$R/H^*(cv/ch)^{0.5}$	x	ch	cv	T50 3D	$R/H^*(cv/ch)^{0.5}$	x	ch	cv	T50 3D	$R/H^*(cv/ch)^{0.5}$	x
0.15	#DIV/0!	0.0000	#DIV/0!	0.0000	#DIV/0!	#DIV/0!	#DIV/0!	#DIV/0!	#DIV/0!	#DIV/0!	#DIV/0!	#DIV/0!	#DIV/0!	#DIV/0!	#DIV/0!	#DIV/0!	#DIV/0!	#DIV/0!	#DIV/0!	13.3401	#DIV/0!	#DIV/0!
6.54	#DIV/0!	0.0000	#DIV/0!	6.2635	#DIV/0!	#DIV/0!	#DIV/0!	#DIV/0!	#DIV/0!	#DIV/0!	#DIV/0!	#DIV/0!	#DIV/0!	6.3226	#DIV/0!	#DIV/0!	#DIV/0!	#DIV/0!	#DIV/0!	#DIV/0!	#DIV/0!	#DIV/0!
12.92	#DIV/0!	0.0000	#DIV/0!	11.5191	#DIV/0!	#DIV/0!	#DIV/0!	#DIV/0!	6.2241	#DIV/0!	#DIV/0!	#DIV/0!	#DIV/0!	5.8932	#DIV/0!	#DIV/0!	#DIV/0!	#DIV/0!	#DIV/0!	1.8732	#DIV/0!	#DIV/0!
25.7	101.8690	62.8920	0.5009	4.8994	0.0024	0.2269	4.8726	23.8730	6.7931	0.0033	0.2743	3.3333	22.6436	0.3231	0.0002	0.0642	60.8552	19.6622	1.0439	0.0005	0.0956	27.4378
48.44	136.0384	62.5625	0.5035	7.5296	0.0027	0.2462	4.1823	31.4913	9.0656	0.0033	0.2742	3.3712	30.5617	0.9364	0.0003	0.0810	38.6020	36.1469	#DIV/0!	#DIV/0!	#DIV/0!	#DIV/0!
96.73	140.4265	61.7800	0.5099	7.2095	0.0025	0.2357	4.6796	33.7372	9.1026	0.0032	0.2698	3.5707	32.5024	5.6571	0.0020	0.2045	6.2134	35.1498	5.3204	0.0019	0.2000	6.4993
193.32	143.1263	60.4250	0.5213	5.3498	0.0018	0.1957	7.0959	37.9616	8.1202	0.0028	0.2497	4.3573	35.3824	10.7576	0.0037	0.2944	3.1351	33.7262	10.6294	0.0036	0.2905	3.2214
386.49	102.5428	58.1750	0.5415	5.9372	0.0028	0.2527	4.5913	27.2595	12.8988	0.0062	0.4127	1.7210	22.1987	4.8192	0.0023	0.2239	5.8501	28.1924	6.7916	0.0032	0.2710	3.9921
772.83	54.1921	54.4500	0.5785	7.0849	0.0064	0.4245	1.8572	13.1585	9.5546	0.0086	0.5288	1.1967	11.4337	7.3148	0.0066	0.4345	1.7727	12.9669	8.7823	0.0079	0.4954	1.3637
1545.51	75.5968	49.9500	0.6306	8.0212	0.0052	0.3662	2.9656	23.7876	12.0496	0.0078	0.4913	1.6480	19.8572	7.6877	0.0050	0.3560	3.1382	24.1260	12.9655	0.0084	0.5182	1.4812
3090.88	62.2455	45.3250	0.6950	8.0354	0.0063	0.4206	2.7303	21.9388	10.0982	0.0079	0.4977	1.9501	19.6925	8.2775	0.0065	0.4298	2.6148	21.6443	14.5271	0.0114	0.6471	1.1535

Uncorrected 3D using fc=4 up to standard 60% regions																						
3D Sample 2				1D Sample A				1D Sample B				1D V Perm 1				1D V Perm 2						
Pressure (kPa)	cv,3Dequiv	H	R/H	cv	T50 3D	R/H*(cv/ch)^(0.5)	x	cv	T50 3D	R/H*(cv/ch)^(0.5)	x	cv	T50 3D	R/H*(cv/ch)^(0.5)	x	cv	T50 3D	R/H*(cv/ch)^(0.5)	x			
0.1500	#DIV/0!	0.0000	#DIV/0!	0.0000	#DIV/0!		#DIV/0!	#DIV/0!	#DIV/0!		#DIV/0!	#DIV/0!	#DIV/0!	#DIV/0!		#DIV/0!	13.3401	#DIV/0!		#DIV/0!		
6.5400	#DIV/0!	0.0000	#DIV/0!	6.2635	#DIV/0!		#DIV/0!	#DIV/0!	#DIV/0!		#DIV/0!	6.3226	#DIV/0!		#DIV/0!	#DIV/0!	#DIV/0!	#DIV/0!		#DIV/0!		
12.9200	#DIV/0!	0.0000	#DIV/0!	11.5191	#DIV/0!		#DIV/0!	6.2241	#DIV/0!		#DIV/0!	5.8932	#DIV/0!		#DIV/0!		1.8732	#DIV/0!		#DIV/0!		
25.7000	79.5738	62.8875	0.5009	4.8994	0.0030	0.2619	3.6586	6.7931	0.0042	0.3181	2.4790	0.0002	0.0683	53.8106		1.0439	0.0006		0.1043	23.0484		
48.4400	78.4053	62.5215	0.5038	7.5296	0.0047	0.3428	2.1599	9.0656	0.0057	0.3887	1.6802	0.9364	0.0006	0.1031	23.9005	#DIV/0!	#DIV/0!			#DIV/0!		
96.7300	72.6380	61.5910	0.5114	7.2095	0.0049	0.3503	2.1316	9.1026	0.0061	0.4116	1.5438	5.6571	0.0038	0.3008	2.8915	5.3204	0.0036		0.2905	3.1006		
193.3200	85.0474	60.2700	0.5226	5.3498	0.0031	0.2652	3.8854	8.1202	0.0047	0.3415	2.3419	10.7576	0.0062	0.4144	1.5906	10.6294	0.0061		0.4097	1.6276		
386.4900	47.8835	57.8500	0.5445	5.9372	0.0061	0.4085	1.7769	12.8988	0.0132	0.7347	0.5492	4.8192	0.0049	0.3535	2.3722	6.7916	0.0069		0.4483	1.4755		
772.8300	32.9551	54.2500	0.5806	7.0849	0.0105	0.6099	0.9064	9.5546	0.0142	0.7940	0.5347	7.3148	0.0109	0.6244	0.8648	8.7823	0.0131		0.7293	0.6338		
1545.5100	52.0916	49.6750	0.6341	8.0212	0.0075	0.4789	1.7534	12.0496	0.0113	0.6442	0.9690	7.6877	0.0072	0.4641	1.8670	12.9655	0.0122		0.6837	0.8602		
3090.8800	47.2494	45.0250	0.6996	8.0354	0.0083	0.5152	1.8443	10.0982	0.0105	0.6073	1.3273	8.2775	0.0086	0.5264	1.7664	14.5271	0.0151		0.8540	0.6712		

